



# GLAST Tracker Mechanical Design PDR Design Review Document

Erik Swensen, Steve Ney, Franz Biehl, Edward Romero, Mike Steinzig  
6/5/2001

	Name:	Phone & E-Mail	Signature:
Main Authors:	Erik Swensen, Steve Ney	(505) 661-4021 <a href="mailto:swensen@hytecinc.com">swensen@hytecinc.com</a> (505) 662-0511 <a href="mailto:ney@hytecinc.com">ney@hytecinc.com</a>	
Approved:	Erik Swensen	(505) 661-4021 <a href="mailto:swensen@hytecinc.com">swensen@hytecinc.com</a>	

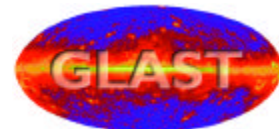
## Abstract

This document provides an overview of the Tracker tower mechanical component design. Design concepts, requirements, material selection, test plans, program plans and costing information are presented in the form of a design review document for PDR. The mechanical design is currently under development; therefore, design details presented herein are current as of PDR only. The work presented in this document is being funded under a DOE/SLAC contract in support of the GLAST project.

DESIGN ENGINEERING  
ADVANCED COMPOSITE APPLICATIONS  
ULTRA-STABLE PLATFORMS

110 EASTGATE DR.  
LOS ALAMOS, NM 87544

PHONE 505 661-3000  
FAX 505 662-5179  
WWW.HYTECINC.COM



## Revision Log

<b>Rev.</b>	<b>Date</b>	<b>Author(s)</b>	<b>Summary of Revisions/Comments</b>
-	June, 2001	ES, SN	Initial release.

## Table of Contents

<b>1. Executive Summary .....</b>	<b>5</b>
<b>2. Definitions.....</b>	<b>6</b>
<b>3. Introduction .....</b>	<b>8</b>
<b>3.1 GLAST General Description.....</b>	<b>8</b>
<b>3.2 Environmental Requirements.....</b>	<b>11</b>
3.2.1 Static Loads .....	11
3.2.2 Dynamic Loads .....	11
3.2.3 Structural Stiffness.....	13
3.2.4 TKR Tower Alignment .....	15
3.2.5 Thermal Loads .....	15
3.2.6 Launch Pressure.....	16
3.2.7 Venting.....	16
3.2.8 EMI Protection.....	16
3.2.9 Outgassing and Contamination .....	16
3.2.10 Tower Handling .....	16
3.2.11 Radiation Length.....	16
<b>4. Material Selection .....</b>	<b>17</b>
4.1.1 Tray Closeout Frame Material Selection.....	17
4.1.2 Tray Sandwich - Core Material Selection .....	17
4.1.3 Tray Sandwich - Face Sheet Material Selection .....	20
4.1.4 Tower Sidewall Material Selection .....	22
<b>5. Tracker Mechanical Design Concept.....</b>	<b>24</b>
<b>5.1 Tracker Tray Sandwich Structure Design Concept.....</b>	<b>24</b>
5.1.1 Standard Tray Configuration With/Without Converter Foil.....	24
5.1.2 SuperGLAST Tray Configuration .....	26
5.1.3 Top/Bottom Tray Configuration .....	27
5.1.4 Tray Mechanical Performance.....	27
<b>5.2 Tracker Tower Sidewalls .....</b>	<b>29</b>
<b>5.3 Stacked Tray Tracker Tower.....</b>	<b>29</b>
5.3.1 Stacked Tray Design Concept.....	29
5.3.2 Tower Mechanical Performance .....	32
<b>5.4 Mechanical Interfaces for the TKR Tower Mechanical Components.....</b>	<b>35</b>
5.4.1 Internal Interfaces .....	35
5.4.2 External Interfaces .....	36
<b>6. Tracker Thermal Design Concept.....</b>	<b>37</b>
<b>6.1 Thermal Conduction.....</b>	<b>37</b>
6.1.1 Tracker Tray Sandwich Structure.....	37
6.1.2 Stacked Tray Tracker Tower .....	39
6.1.3 Tracker Tower Interfaces .....	44
<b>6.2 Coefficient of Thermal Expansion.....</b>	<b>45</b>
6.2.1 Tracker Tray Sandwich Structure.....	45
6.2.2 Stacked Tray Tracker Tower .....	46
<b>7. Tracker Fabrication and Assembly .....</b>	<b>50</b>
<b>7.1 Sandwich Tray Construction.....</b>	<b>50</b>
<b>7.2 Tracker Stacked Tray Tower Assembly Concept.....</b>	<b>52</b>
<b>8. Mechanical Structure Prototype Testing.....</b>	<b>53</b>
<b>8.1 Component Level Coupon Testing .....</b>	<b>53</b>
8.1.1 3D C-C Closeout Coupon Testing .....	53

8.1.2 Tray Sandwich Structure Face Sheets ..... 54

8.1.3 Tower Module Sidewall Coupon Testing..... 55

**8.2 Subsystem Level Prototype Testing ..... 56**

8.2.1 Tray Level Prototype Testing..... 56

8.2.2 Tower Level Prototype Testing ..... 57

***9. Cost for Tracker Tower Mechanical Components ..... 59***

***10. Program Plan..... 60***

***11. References ..... 62***

## 1. Executive Summary

HYTEC is responsible for the thermal-mechanical design of the Tracker (TKR) tower structural components used on the GLAST satellite. Considerable progress has been made on the design to meet project schedule and milestones. Preliminary fabrication drawings have been completed for most of the mechanical hardware, and have been sent to vendors to obtain preliminary pricing information. Some coupon testing and mechanical prototyping has been done to begin validating the design, fabrication, and assembly concepts. The near term objective is to fabricate ten mechanical prototypes and perform tray and tower level testing at qualification levels. Prototyping began in April 2001 and will be followed by fit, form and function testing beginning in July 2001 and qualification/validation testing of the trays and tower in August/September 2001. Our program plan calls for fabrication of the Engineering Model (E/M) prototype to begin June 2001, with qualification level testing in April 2002.

Several modifications have been incorporated into the design since the Beam Test Engineering Model (BTEM) prototype. The primary improvement was the introduction of carbon fiber reinforced composites (CFRC) into the design to enhance performance, but maintain the structural integrity of the TKR tower structural components. Sandwich structures using aluminum core material have been incorporated into the design, which greatly reduces the cost with minimal impact on performance. Tray fabrication and tower assembly procedures have been modified to improve dimensional repeatability and simplify tower assembly.

A testing program was approved in August 2000 to validate design concepts at a coupon level, tray level, and tower level prior to E/M fabrication. This allows us to resolve difficult fabrication and design issues prior to E/M prototype fabrication and testing.

The schedules have been modified to bring the TKR tower mechanical component fabrication in line with SSD delivery. The FY'01 schedule has slipped by 6-8 weeks because of long lead times for material procurement, but does not impact E/M and Flight hardware delivery schedules.

## 2. Definitions

ACD:	Anti-Coincidence Detector subsystem
Al:	Aluminum
ASD:	Acceleration Spectral Density
BTEM:	Beam Test Engineering Module
CAD:	Computer Aided Design
CAL:	Calorimeter subsystem
C-C:	Carbon-Carbon Material
CDR:	Critical Design Review
CsI:	Cesium Iodide
CTE:	Coefficient of Thermal Expansion
CVCM:	Collected Volatile Condensable Material
DoF's:	Degrees-of-Freedom
dB:	Decibel
E/M:	Engineering Model
EMI:	Electro-magnetic Interference
FEA:	Finite Element Analysis
FEM:	Finite Element Modeling
GEVS:	General Environmental Verification Specification
GFRC:	Graphite Fiber Reinforced Composite
GFRP:	Graphite Fiber Reinforced Plastic
GLAST:	Gamma-ray Large Area Space Telescope
Gr/CE:	Graphite/Cynate Ester
IRD:	Interface Requirements Document
LV:	Launch Vehicle
MECO:	Main Engine Cutoff
PDR:	Preliminary Design Review
Q:	Quality Factor
RL:	Radiation Length
RMS:	Root-Mean-Square
SBIR:	Small Business Innovative Research

SI:	Science Instrument
SI-SC:	Science Instrument-Spacecraft
SSD('s):	Silicon Strip Detector(s)
T&DF:	Trigger & Dataflow subsystem
TMCM:	Tracker Multi-Chip Modules
TML:	Total Material Loss
TKR:	Tracker subsystem
WBS:	Work Breakdown Structure

### 3. Introduction

HYTEC is responsible for the thermal-mechanical design of the TKR tower mechanical components. The major elements include the honeycomb sandwich structure, which supports the silicon strip detector (SSD) payload, and the stacked tray tower assembly concept. This document reviews the progress made to date in preparation for the TKR PDR.

#### 3.1 GLAST General Description

Figure 1 shows a CAD rendering of the GLAST science instrument (SI). The primary subsystems are shown as they are configured in the instrument package. The SI consists of an Anticoincidence Device (ACD), a silicon-strip detector tracker, a hodoscopic CsI calorimeter (CAL), and a Trigger and Dataflow subsystem (T&DF). The principle purpose of the SI is to measure the incidence direction, energy, and time of cosmic gamma rays. The measurements are streamed to the spacecraft for data storage and subsequent transmittal to ground-based analysis centers.

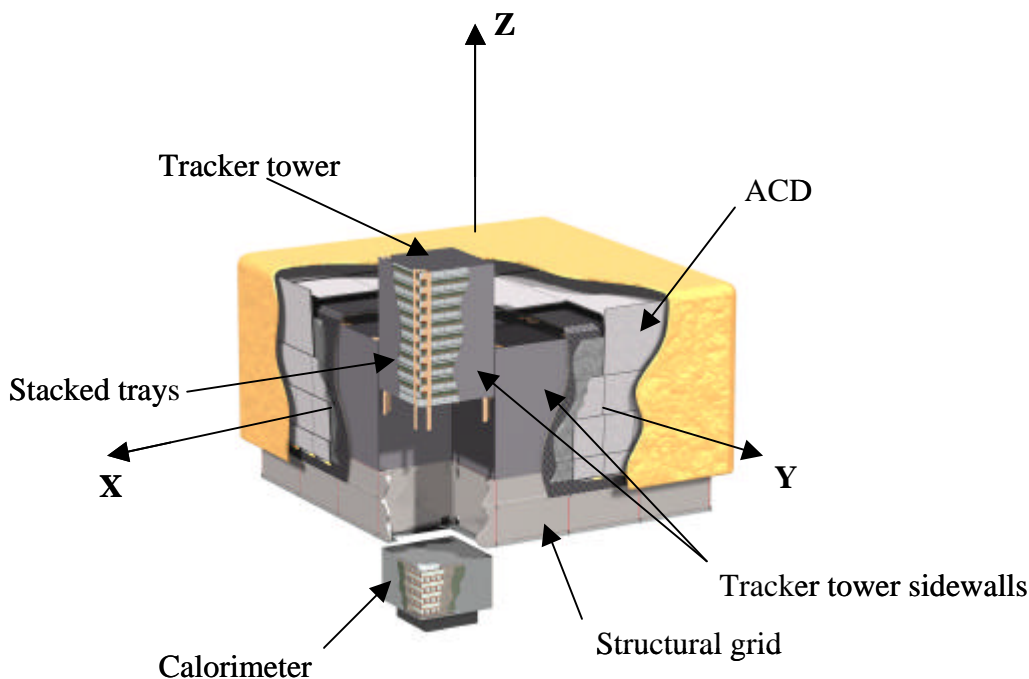


**Figure 1. CAD rendering of the GLAST satellite. The primary subsystems are shown with emphasis on the TKR components.**

The SI is designed and arranged in a modular 4x4 array of 16 tower assemblies; closely spaced (1.5mm gaps) to minimize inactive areas within the telescope footprint, but allow dimensional changes that will result from environmental and assembly effects. The space between towers will allow for: 1) thermal expansion of the aluminum grid relative to the composite TKR; 2) relative positioning errors that result from fabrication, assembly and alignment tolerances; 3) deflections that result from both static and dynamic inputs present within the launch environment; 4) EMI shielding between TKR towers. Each tower assembly consists of one CAL, supported

inside of the grid, and one TKR tower, supported on top of the grid, mounted directly above a CAL. The 16 TKR towers are enclosed by the ACD, which is supported around its perimeter by the grid.

The TKR converts gamma rays to charged particles and measures with great precision the path of the charged particles within the TKR. Fast signals from tracks are examined in the T&DF subsystem for likely gamma ray candidates. Once identified and at the request of the trigger system, data is read out via a dataflow system. The dataflow system uses the data to assemble particle tracks and, coupled with the ACD and CAL, identify gamma rays.

Each TKR tower module is made up of 19 trays that support the SSD's, bias-circuitry, tungsten converter foils, and Tracker Multi-Chip Modules (TMCM), as shown in Figures 2 and 3; the term TKR tower module will be referred to as simply the TKR tower for the remainder of this document. Each tray supports 16 SSD's on both the upper and lower surfaces of the tray, with the exception of the top and bottom trays, which support 16 SSD's on one surface only. The top 12 trays support 3% of a radiation length (RL) of tungsten converter foil on their lower surfaces. The next four trays support 18% of a RL of tungsten converter foil. The last three trays support the standard payload on both surfaces without the tungsten converter foil. The bottom tray supports the SSD payload on one surface only. The trays are subsequently stacked with adjacent trays rotated 90° to form an x-y detector plane immediately below the converter foil. The TKR tower is completed with all 19 trays supported on four sides with thermal/mechanical sidewalls. The TKR tower is mounted to the aluminum grid using flexure mounts, shown in Figure 4, to account for the CTE mismatch between the Al grid and GFRC tower. A thermal gasket is proposed to transfer heat from the TKR tower into the grid, and subsequently into the radiators, with minimal shear load transfer.

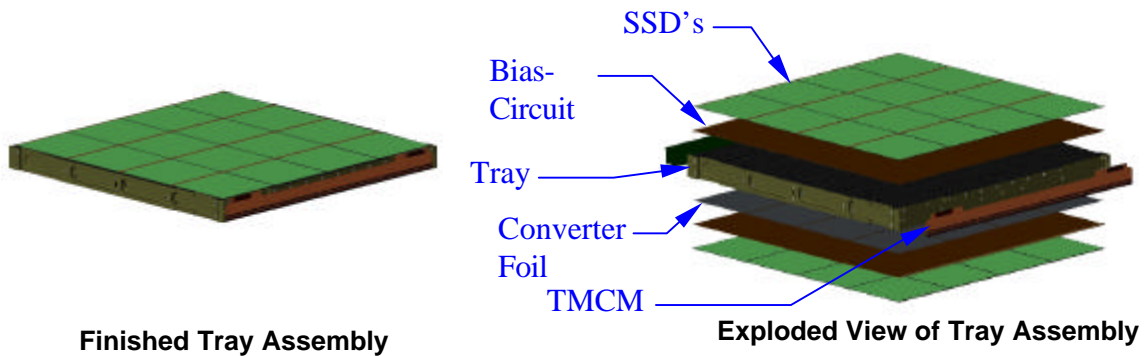


**Figure 2. Standard TKR tray showing the SSD's, bias-circuitry, tungsten converter foils, and TMCM's.**

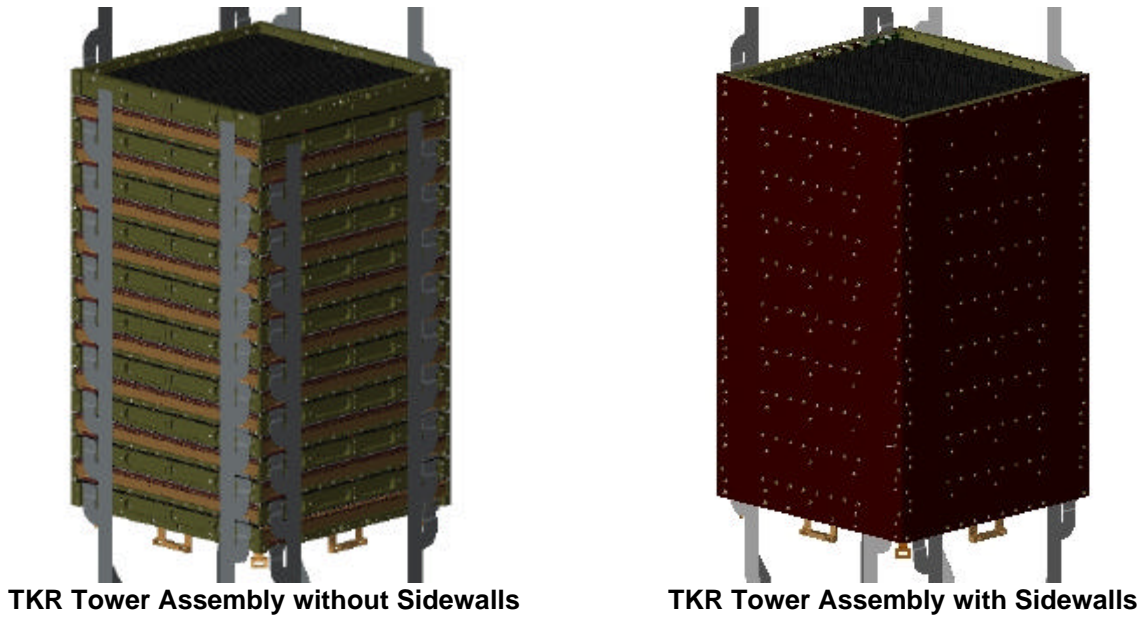


**Figure 3. TKR tower showing all 19 trays with the sidewalls removed and installed.**

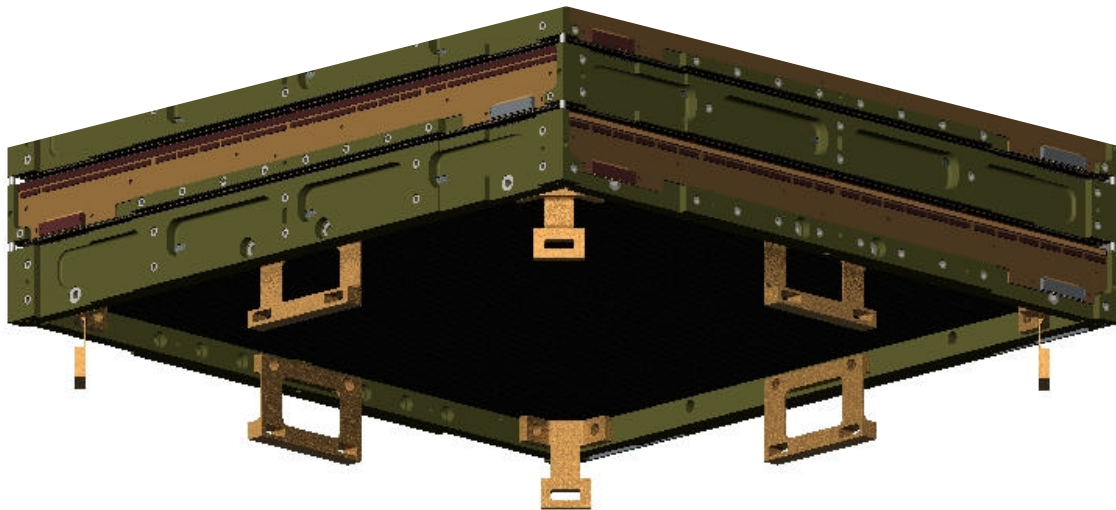


**Figure 4. Bottom tray-to-grid flexure mounting concept.**

This report details the TKR tower thermal/mechanical design concepts to be presented at the PDR. Mechanical components are described in detail with supporting analysis and testing outlined. Development of the design concepts presented herein will continue through CDR and design modifications will be incorporated as required.

### 3.2 Environmental Requirements

*References: LAT-SS-00134, GLAST SI-SC IRD, NASA GEVS (Rev. A), Delta II Payload Planners Guide, NASA-STD-5001*

The design requirements presented in this section are a consolidation of the key design requirements used to develop the TKR structural components. Design limit loads are defined in the *LAT TKR Detailed Subsystem Specification – Level IV Specification (LAT-SS-00134)*. Alternate applicable documents include the GLAST SI-SC IRD, NASA GEVS (Rev. A), and the Delta II Payload Planners Guide. Margins of Safety will be computed using factors from the NASA-STD-5001 standards document.

#### 3.2.1 Static Loads

Static load requirements are given in the SI-SC IRD, section 3.2. The IRD requires that the design of SI primary structures shall use the quasi-static limit load factors listed in Table 1, applied at the center of gravity of the SI. Loads are given in units of gravitational acceleration,  $g = 9.81\text{m/s}^2$ . Qualification level design loads are computed using a factor of 1.25 to the quasi-static design loads, and are listed in Table 2.

**Table 1. Quasi-Static design limit loads for SI primary structures.**

Axis	Liftoff/Transonic	MECO
Thrust	+ 3.25 / - 0.8	+ 6.0 ± 0.6
Lateral	± 4.0	± 0.1
<ul style="list-style-type: none"> <li>• + indicates compression</li> <li>• loads are in g's</li> </ul>		

**Table 2. Qualification level quasi-static design limit loads for SI primary structures.**

Axis	Liftoff/Transonic	MECO
Thrust	+ 4.06 / - 1.0	+ 8.25
Lateral	± 5.0	± 0.125
<ul style="list-style-type: none"> <li>• + indicates compression</li> <li>• loads are in g's</li> <li>• These loads are computed from a factor of 1.25 x Design Limit Loads</li> </ul>		

#### 3.2.2 Dynamic Loads

The SI-SC shall be subjected to several dynamic sources during launch. These sources include random vibrations, acoustic emissions and pyroshock from the Delta II launch vehicle. NASA's GEVS provides dynamic specifications for each of these sources in addition to other load requirement information. At the time of this writing, GEVS levels were being used in all analysis and testing. These levels will eventually be replaced with Delta II response spectra, where applicable.

##### 3.2.2.1 Random Vibrations

Random vibration levels are specified in the GEVS, section 2.4 – “Structural and Mechanical,” paragraph 2.4.2.5 – “Component/Unit Vibroacoustic Tests,” sub-paragraph (a) –

“Random Vibration.” The SI and components are required to withstand random vibration levels that meet or exceed the levels outlined in Table 3 along each of three mutually perpendicular axes for one minute (where applicable). The table gives exact qualification and acceptance test level Acceleration Spectral Density (ASD) functions, given in  $g^2/Hz$ , for components weighing 22.7 kg. Qualification levels are defined as the flight limit level, acceptance, plus 3 dB. The table also specifies that the ASD levels may be reduced using the equations provided for components weighing more than 22.7 kg. GEVS also allows for the input spectrum to be notched around SI fundamental frequencies.

**Table 3. Generalized random vibration test levels for components (STS or ELV) weighing 22.7 kg (50 lbs) or less.**

Frequency (Hz)	ASD Level ( $g^2/Hz$ )	
	Qualification	Acceptance
20	0.026	0.013
20-50	+6 dB/oct	+6 dB/oct
50-800	0.16	0.08
800-2000	-6 dB/oct	-6 dB/oct
2000	0.026	0.013
Overall	14.1 $g_{rms}$	10.0 $g_{rms}$

The acceleration spectral density level may be reduced for components weighing more than 22.7 kg (50 lbs) according to the following:

	<u>Weight in kg</u>	<u>Weight in lbs</u>	
dB Reduction	$= 10 \log(W/22.7)$	$10 \log(W/50)$	
ASD(50-800 Hz)	$= 0.16 (22.7/W)$	$0.16 (50/W)$	for protoflight
ASD(50-800 Hz)	$= 0.08 (22.7/W)$	$0.08 (50/W)$	for acceptance

Where W = component weight.

The slopes shall be maintained at + and – 6 dB/oct for components weighing up to 59 kg (130 lbs). Above that weight, the slopes shall be adjusted to maintain an ASD level of 0.01  $g^2/Hz$  at 20 and 2000 Hz.

For components weighing over 182 kg (400 lbs), the test specification will be maintained at the level for 182 kg (400 lb).

Figure 5 illustrates the ASD levels detailed in the GEVS and indicates the maximum, minimum and transition plots.

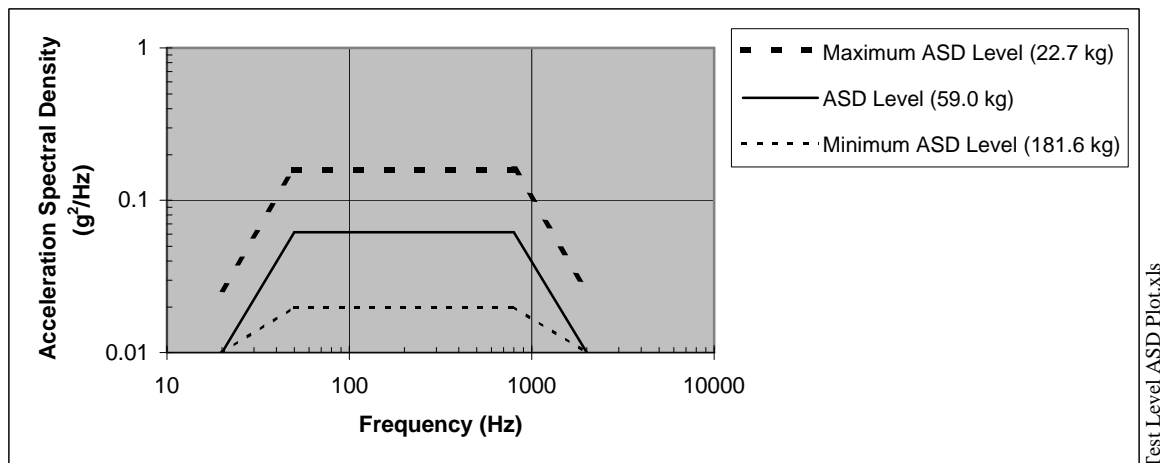


**Figure 5. Generalized Random Vibration Test Levels for the Shake Test 99 Calorimeter.**

### 3.2.2.2 Acoustic Loads

Acoustic loads are assumed to act on the ACD during launch. These loads are considered to have little effect on the TKR itself. Should acoustic load analyses for the ACD show that significant forces are transmitted to the TKR, such loads will be taken into consideration in subsequent TKR analyses. Analysis has not been performed, but testing is planned.

The completed TKR tower shall be qualified for the qualification noise levels defined in GEVS Table D-3.

### 3.2.2.3 Pyroshock Loads

Pyroshock loads are considered negligible at the TKR interface. Pyroshock levels are reduced at locations away from the source. Attenuation of the input levels is effected by transmission distance and transmission through mechanical joints. Considering these knockdown factors, the input levels at the TKR interface will be less than 2% of the source input, considering 90% knockdown from distance and 40% knockdown through each bolted joint (up to 3). Analysis has not been performed, but testing is planned.

The TKR shall be capable of normal operation after the application of the external shock levels applied at the spacecraft separation ring interface, at levels defined in GEVS Tables D-8 or D-9.

### 3.2.3 *Structural Stiffness*

The IRD has defined minimum requirements for the fixed base stiffness for the SC-SI. The fixed base stiffness of the SI-SC system shall produce a first mode frequency greater than 35 Hz in the thrust direction, and greater than 12 Hz in the lateral direction. These values are based on the measured response of the Delta II launch vehicle and are selected to avoid dynamic coupling between the low-frequency launch vehicle and spacecraft modes.

Increased stiffness values will be required at the component level. Minimum design values have been determined from finite element analyses (FEA) for the TKR components. Table 4 summarizes the design value stiffness requirements of each individual component, where applicable.

**Table 4. Summary of Component Level Stiffness Requirements.**

SI-SC System Components	Fixed Base – Fundamental Frequency
SI-SC	<ul style="list-style-type: none"> <li>• &gt; 35 Hz in the Thrust Direction</li> <li>• &gt; 12 Hz in the Lateral Direction</li> </ul>
Science Instrument	
ACD	• Not Applicable
Tracker	
Tower	• > 100 Hz goal in the Lateral and Thrust Direction
Tray	<ul style="list-style-type: none"> <li>• &gt; 500 Hz in the Thrust Direction</li> <li>• N/A in the Lateral Direction</li> </ul>
Calorimeter	• Not Applicable
Grid	• > 50 Hz goal in the Thrust Direction with TKR stiffness included

### 3.2.3.1 SI-SC Stiffness

This requirement was specified in the IRD to avoid coupling the response of the SI-SC with the response of the launch vehicle (i.e. coupled natural frequencies).

### 3.2.3.2 Tracker Stiffness

TKR stiffness is considered for response to static and dynamic loads. Additionally, the TKR may be affected by coupling with the ACD and structural grid of the SI.

#### 3.2.3.2.1 Tower Stiffness

Tower stiffness requirements are defined by the requirement that the towers do not collide or experience excessive loads or stresses, maintaining acceptable Margin of Safety when subjected to the aforementioned load conditions.

At the time of this writing, the fixed base stiffness must be sufficient to provide a minimum fundamental frequency of 100 Hz. This will be reviewed to ensure that the requirements of paragraph 1 are maintained.

#### 3.2.3.2.2 Tray Stiffness

The tray stiffness requirement was derived from the 2 mm separation requirement between XY-pairs of SSD's. During normal operations, the separation requirement will not present any difficulties. However, during launch conditions, excessive vibrations in the trays can cause collisions between two adjacent trays, likely causing damage to SSD's or tray structural components. To reduce the risk of damaging collisions, a minimum stiffness requirement of 500 Hz has been derived using a fixed-base boundary condition. This frequency requirement assumes that there is a 5% probability that one peak will exceed collision levels during the 60 second qualification test duration, and adjacent trays are assumed to be 180° out-of-phase. A quality factor (Q) of 40 is assumed until tests prove otherwise.

### 3.2.3.3 Calorimeter Stiffness

The CAL stiffness is not considered in any TKR analysis.

### 3.2.3.4 ACD Stiffness

The ACD stiffness is not considered in any TKR analysis.

### 3.2.3.5 Grid Stiffness

The Grid stiffness has a direct effect on the tower-to-tower relative response. However, all TKR development presented herein assumes a fixed base boundary condition at the Grid-to-TKR interface, thereby neglecting Grid stiffness effects. System level response is outside the scope of TKR development work presented here.

### 3.2.4 TKR Tower Alignment

The TKR tower shall maintain a lateral alignment within the 300  $\mu\text{m}$  tower alignment stay-out-zone. This means that there is 150  $\mu\text{m}$  on each side of the tower to allow for alignment drift.

### 3.2.5 Thermal Loads

TKR thermal loads are generated by tray electronics. It is assumed that thermal loads due to incident and reflected radiation, as well as convection, are negligible for the TKR subassembly. The following section describes thermal loads that affect the TKR through conduction.

#### 3.2.5.1 Tower Thermal Requirements

The TKR tower shall not exceed a maximum operating temperature of +25°C during normal operating conditions. A temperature gradient along the length of the tower will vary the tray temperatures, with the maximum temperature being at the top of the tower. The maximum temperature drop from the top tray to the Grid interface shall be no more than -12°C, assuming no more than 0.35 W of power dissipation per TCM.

#### 3.2.5.2 Environmental Temperature and Humidity Requirements

The TKR thermal and humidity requirements are governed by the requirements for the entire SI. Table 5 shows the temperature maximum and minima, maximum rate of temperature change and humidity constraints for the current design.

**Table 5. Thermal and humidity requirements for the GLAST SI.**

	SI Temp Ranges		Environmental Temperatures			
	Operational	Survival	Storage	Integration <sup>(2)</sup>	On LV <sup>(2)</sup>	Launch <sup>(2)</sup>
T <sub>max</sub> test <sup>(1)</sup>	35°C	50°C				
T <sub>max</sub> design	25°C	40°C	40°C	25°C	26.7°C	30°C
T <sub>min</sub> design	-10°C	-20°C	0°C	15°C	12.8°C	0°C
T <sub>min</sub> test <sup>(1)</sup>	-20°C	-30°C				
dT/dt <sub>max</sub> <sup>(3)</sup>		5 °C/hr				
Humidity			20 - 55%	35 - 55%	40 - 55%	40 - 55%
<sup>(1)</sup> Test temperature set at 10 °C higher than maximum design temperature, and 10 °C lower than minimum design temperature, per GEVS-SE rev A <sup>(2)</sup> Temperature ranges per Delta II Payload Planner's Guide <sup>(3)</sup> Maximum time rate of change of temperature						

### *3.2.6 Launch Pressure*

The TKR tower shall withstand the time rate of change of pressure in the launch vehicle fairing shown in the Delta II Payload Planner's Guide, Section 4.2.1, Figure 4.2.

### *3.2.7 Venting*

Sufficient venting of all TKR components is required to allow trapped gasses to release during launch. Venting paths must be large enough to minimize pressure differentials within tray structures and tower assemblies. This includes adequate venting of the honeycomb core and inner tower enclosed spaces. Gasses shall vent into other subsystems, therefore gas volumes and rates must be communicated with other subsystems.

### *3.2.8 EMI Protection*

Each TKR tower shall be covered on all 6 sides by at least 50  $\mu\text{m}$  of aluminum electrically connected to the Grid.

### *3.2.9 Outgassing and Contamination*

Spacecraft materials may be accepted or rejected based on the basis of outgassing and/or contaminants released. The following sections describe design constraints on selected TKR materials.

#### *3.2.9.1 Outgassing*

All materials used in the TKR shall meet the NASA outgassing requirements. Values of 1.00% and 0.10% have been used historically as screening levels for rejection based on TML and CVCM, respectively. We will reject TKR materials which exceed either of these amounts, unless screening levels are expanded by those in charge of SI requirements.

#### *3.2.9.2 Contamination*

SI contamination is caused by particulates generated from materials, machining and assembly procedures. Care will be taken to keep contamination to a minimum.

All machined carbon-carbon surfaces to which adhesives will not be applied shall be coated with  $\geq 2 \mu\text{m}$  of polymer to prevent the release of carbon dust. The cut edges of face sheets and tower sidewalls shall be filleted with cyanate ester resin, or equivalent, to prevent the release of carbon fiber fragments. Trimming and grinding of completed tray panels will be prohibited during tray and tower assembly.

### *3.2.10 Tower Handling*

The top tray of each TKR tower shall include special attachment points for handling during integration into the SI. These points will allow lifting from the top without interference from adjacent towers, and must support the mass of the TKR tower.

### *3.2.11 Radiation Length*

The TKR tower module mechanical components must provide a minimum radiation length solution. Long radiation length materials along with optimum design concepts are required.

## 4. Material Selection

Material Selection for the GLAST TKR is divided into four mechanical sub-components: Tray Closeout Frame, Tray Sandwich Structure Core, Tray Sandwich Face Sheets, and Tower Sidewalls. A matrix study was done comparing composite versus conventional materials, where applicable. The matrix studies considered mechanical and dynamic strength, thermal properties, and cost as well as availability, flight history, and overall compatibility with other materials selected for the other major sub-components.

### 4.1.1 Tray Closeout Frame Material Selection

Material Selection for the TKR tray closeout frame evolved from the aluminum frame concepts used on the BTEM to the 3D C-C frame concepts selected for the E/M and flight hardware. The original aluminum frames have a shorter RL, so GFRC's were explored as an alternative. Graphite fiber reinforced plastics (GFRP) [epoxy based] composites were initially investigated using high-end fibers to meet thermal and structural requirements. Unfortunately, high-end carbon fibers that have the high thermal conductivity necessary to meet GLAST constraints are too expensive to meet budgetary constraints. Low-end carbon fibers do not meet the thermal conductivity requirements, so alternative GFRC's were considered. A 3D C-C composite was investigated that has the necessary thermal conductivity and structural strength to meet GLAST constraints at an affordable cost.

A 3D C-C material refers to a carbon fiber based material that is supported by a carbon matrix. The initial approach was to use recycled C-C brake shoe material that was heat-treated to improve the thermal conductivity and resin re-impregnated to improve mechanical strength. This material provided the thermal conductivity, strength and long radiation length necessary to meet the requirements and goals of the GLAST project, at an affordable price. One drawback with this material was the limited size of available material. The material only came in a donut shape and the net harvest was half a single closeout wall, with too much scrap. As a result, a virgin form of this material has been under development to reduce the amount of scrap and allow for a single closeout wall to be machined from a rectangular blank of 3D C-C. The results are promising and the material is being manufactured in virgin form and used in tray prototypes. The strength and modulus tests gave promising results, although the initial tests indicated a higher level of porosity in the material and a lower flexural strength. This is currently being corrected and future performance is expected to improve.

### 4.1.2 Tray Sandwich - Core Material Selection

*Reference: HTN-102060-0001*

The honeycomb core used in both the standard and superGLAST TKR tray sandwich structures plays a critical role for improving the dynamics of the TKR tower. For this reason, the core material would need to be exceptionally light with high shear strength and have a reasonably long radiation length. Three base materials were considered: GFRC, aluminum, and Kevlar fiber reinforced composites. Standard fibers were considered for the different composites to ensure availability and keep prices reasonable.

In selecting the core material and geometry, the following requirements were considered to assess the core performance.

- Mass: the NASA proposal, issued November 1999, assumed a core mass of ~123 grams.
- Radiation Length: 0.2% of a radiation length was used in Monte Carlo simulations performed for the NASA proposal.
- Tray Stiffness: a fundamental frequency of 500 Hz ( $Q = 40$ ), was used as the minimum design value to avoid collision between adjacent trays during qualification level random vibration excitation.
- Mechanical Loading: two combinations of pseudo-static launch load factor cases were considered, as defined in the GLAST SI-SC IRD,
  - 4.00  $g_y$  and 3.35  $g_z$  (liftoff & transonic)
  - 0.10  $g_y$  and 6.60  $g_z$  (MECO)
- Thermal Requirements: the thermal environment is generally mild, with temperature ranges of  $-20$  to  $+40^\circ\text{C}$ . The CTE mismatch between the aluminum core and GFRP face sheets is considered negligible; similar tray configurations have been prototyped and tested to greater extremes without evidence of damage. The CTE mismatch effects to the payload are also neglected because in-plane stiffness of the core has almost no effect on the thermal stresses induced in the silicon payload.
- Cost: the NASA proposal used a value of \$800/core for the budgetary estimates for fabrication of the flight hardware.
- Venting: the core must be properly vented to allow trapped air to escape during launch.

Table 6 lists the manufacturers of the six honeycomb cores selected. Here, the performance characteristics of the various core materials are compared.

The Kevlar and heavier aluminum cores were ruled out because of poor performance. All the GFRP cores meet program requirements with the exception to cost. Both the UCF-51 and UCF-146 cores exceed the NASA proposal budget by more than 50%. The lighter core meets the cost budget, but has little history and will require some development to ensure success. The thin walled aluminum core, 3/8-5056-0.0007, meets the requirements of the GLAST program and will save the program nearly \$214K. There are remaining technical issues, such as handling and galvanic corrosion, that will be addressed by vendor fabrication experience. Assuming there are no unforeseen issues with the thin walled aluminum core, it is believed that this core will perform to an acceptable level for the standard TKR tray on the GLAST instrument. Further FEA has shown that the heavier aluminum core should perform to an acceptable level for the Super GLAST TKR trays.

**Table 6. Summary table of the standard tray key performance characteristics for various cores.**

	NASA Proposal (Spec's)	YLA Cellular			Hexcel		
		UCF-146 (YSH-70 Fiber)	UCF-126 (YSH-50 Fabric)	UCF-51 (XN-50 Fabric)	3/8-5056- .0007 (Al)	3/8-5056- .002 (Al)	HRH-10- 3/8-3.0 (Kevlar)
<b>Mass</b>							
Density (kg/m <sup>3</sup> )	-	12.04	32.1	32.1	16.05	48.16	48.16
Est. Mass/Core (grams)	123	43	113	113	57	170	170
<b>Stiffness</b>							
Shear Modulus (ksi)	-	14-20	62	60	15	43	6.5
Compressive Modulus (ksi)	-	2	25	34	15	92	17
Fundamental Frequency (Hz)	500	615 <sup>1</sup>	648	672	610	632	480
RMS Displacement (µm)	116	86.7	78.9	75	87.0	81.8	125.4
<b>Radiation Length</b>	0.20%	0.077%	0.21%	0.21%	0.18%	0.54%	NI*
<b>Cost Per Core<sup>2</sup></b>	\$800	\$697	\$1,339	\$1,766	\$80	\$100	NI*
(Top – E/M \$, Bottom – Flight \$)	\$800	\$618	\$1,237	\$1,541	\$50	\$62	NI*
<b>Availability (ARO)</b>	-	6-12 wks	6-12 wks	3-6 wks	7 wks	7 wks	NI*
<b>Flight Heritage</b>	-	None	Limited	Yes	Yes	Yes	NI*
<b>Fabrication/Handling</b>	-	Acceptable	Good	Good	Concern	Good	NI*
<b>CTE Mismatch</b>	-	Ok	Ok	Ok	Ok	Ok	NI*
<b>Venting</b>	Yes	Yes	Yes	Yes	Available	Available	NI*
<b>Galvanic Corrosion</b>	-	None	None	None	Concern	Concern	NI*

\* NI – Not Investigated

<sup>1</sup> Assuming 14 ksi shear modulus.

<sup>2</sup> The aluminum Hexcel cores include the cost for materials, venting and machining tolerances to ±0.001 through the thickness. Manufacturer quotes were used for materials and venting, whereas machining costs were estimated to be 25% greater than the material costs.

#### 4.1.3 Tray Sandwich - Face Sheet Material Selection

*Reference: HTN-102060-0004*

The TKR tray face sheets along with the tray core provide most of the tray structural stiffness. Originally, both aluminum and Gr/CE materials were considered as possible candidates for the face sheets. However, Gr/CE materials were selected because of the distinct advantages they have over aluminum. Gr/CE has a longer RL than aluminum making it more transparent to high-energy particles. In addition, the similar CTE properties for both the 3D C-C closeout frame material and Gr/CE materials make Gr/CE face sheets a better match to the closeout frame.

In selecting the face sheet material from the dozens of different fiber and resin combinations available, the following requirements were used to assess the performance of each face sheet material selected. These requirements are similar to those used in the selection of the core material due to the coupled interaction of both needed to determine static and dynamic tray response.

- Mass: the NASA proposal, issued November 1999, assumed the mass for two face sheets to be 120 grams.
- Radiation Length: a radiation length of 0.1% was assumed for each face sheet in the NASA proposal simulations. (0.1% RL translates into ~188 $\mu$ m thick GFRP face sheet)
- Tray Stiffness: a fundamental frequency of 500 Hz ( $Q = 40$ ), was used as the minimum design value to avoid collision between adjacent trays during qualification level random vibration excitation.
- Mechanical Loading: two combinations of pseudo-static launch load factor cases were considered, as defined in the GLAST SI-SC IRD,
  - 4.00 gy and 3.35 gz (liftoff & transonic)
  - 0.10 gy and 6.60 gz (MECO)
- Cost: the NASA proposal assumed \$50/facesheet and was later adjusted to a cost of \$250/facesheet for the flight hardware budgetary estimates.

Table 7 lists the manufacturers of the three graphite fiber reinforced composites selected. Here, the performance characteristics of the various face sheet materials are compared.

**Table 7. Summary table of GLAST Standard Tray Face sheet Performance Characteristics.**

	NASA Proposal (Spec's)	M55J/954-3 (M55J – Toray PAN Fiber)	XN50/RS-3 (XN50 – Nippon Pitch Fiber)			YSH50/RS-3 (YSH50 – Nippon Pitch Fiber)		
<b>Minimum Ply Thickness (mm)</b>	-	63.5 (0.0025 in.)	38.1 (0.0015 in.)		63.5 (0.0025 in.)	38.1 (0.0015 in.)		63.5 (0.0025 in.)
<b>Number of Plies</b>	-	4	4	6	4	4	6	4
<b>Laminate Thickness (mm)</b>	188	254	152	229	254	152	229	254
<b>Mass</b>								
Density (kg/m <sup>3</sup> )	-	1623	1760	1760	1760	1750	1750	1750
Est. Mass/Laminate (grams)	60	62	40	60	67	40	60	67
<b>Face sheet Stiffness</b>								
Fiber Volume Fraction (%)		60	60	60	60	60	60	60
Tensile Modulus (GPa)	-	113	108	108	108	109	109	109
Fundamental Frequency <sup>3</sup> (Hz)	500	677	591	636	666	593	637	667
RMS Displacement <sup>3</sup> (μm)	116	74.7	91.3	82.0	76.6	90.9	81.8	76.4
<b>Radiation Length per Laminate</b>	0.1%	0.135%	0.08%	0.12%	0.135%	0.08%	0.12%	0.135%
<b>~Cost Per Laminate</b>	\$250	\$184	\$203	\$259	\$211	\$187	\$235	\$224
<b>Availability (ARO)</b>	-	4 wks	4-8 wks	4-8 wks	4 wks	4-8 wks	4-8 wks	4 wks
<b>Flight Heritage</b>	-	Extensive	Good	Good	Good	Limited	Limited	Limited
<b>Fabrication/Handlin</b>	-	Fair	Fair	Good	Fair	Fair	Good	Fair

Several Gr/CE face sheet options were compared to the NASA proposal baseline based upon general performance characteristics. The thicker laminates exceeded the NASA proposal's requirements for thickness, mass, and radiation length. The only laminate, which exceeded the proposed cost budget, is the six-ply XN50 face sheet. The thin four-ply laminates meet most of the requirements listed in Table 7 for the NASA proposal. Based upon cost, a greater savings could be realized with the use of YSH50 fibers over XN50 fibers. Therefore, the YSH50 1k tow (38.1 μm thickness), unbalanced four-ply lay-up is the better choice for the standard TKR trays in the GLAST instrument.

<sup>3</sup> Based on using Hexcel 3/8-5056-0.0007 (A1) vented core and no payload stiffness in FEA model.

#### 4.1.4 Tower Sidewall Material Selection

The GLAST tower sidewalls provide at least 80% of the stiffness for the TKR tower. They act as large shear panels, which prevent the tower from lateral displacements during launch. The sidewalls also provide a thermal pathway for getting heat out of the tower, into the grid, where it is transferred to radiators through a series of heat pipes. For this reason, materials were selected that had good thermal and structural properties with minimal mass contribution. Good CTE matching was also important because of the large number of fasteners used to attach the sidewalls to the 19 TKR trays. Only GFRC's would meet these requirements, so two candidate panels, P30 C-C and YS-90A/CE, were down-selected from a host of many candidates. The following requirements were set for the sidewalls by the NASA Proposal:

- Thermal: the NASA proposal, issued November 1999, assumed the thermal gradient down the sidewalls to be  $\sim 7^{\circ}\text{C}$  for the tower. After further review of the thermal requirements for the calorimeter and the grid, the thermal gradient for the sidewalls was increased to  $12^{\circ}\text{C}$  due to the additional thermal margin available.
- Radiation Length: for radiation length, the maximum sidewall thickness was set at 1.5mm.
- Tower Stiffness: a minimum fundamental frequency of 100 Hz ( $Q = 40$ ), for the tower during qualification loading.
- Mechanical Loading: two combinations of pseudo-static launch load factor cases were considered, as defined in the GLAST SI-SC IRD,
  - 4.00 gy and 3.35 gz (liftoff & transonic)
  - 0.10 gy and 6.60 gz (MECO)
- Cost: the NASA proposal assumed \$1000/sidewall panel for the flight hardware budgetary estimates.

Table 8 lists the resulting matrix comparison.

**Table 8. Summary table of GLAST Tower Sidewall Performance Characteristics.**

	P30 C/C	YS-90A/CE	Notes:
<b>THERMAL PERFORMANCE</b>			
Kx, Ky, Kz (W/mK)	307,192,12	255,122,2	Measured values
$\Delta T - 1D$ ( $^{\circ}C$ ) (along length/ boss width) <sup>4</sup>	7.4/13.4	8.9/16.1	Calculated values using measured k values COSMOS model
$\Delta T - 2D$ ( $^{\circ}C$ ) <sup>4</sup>	8.7	10.4	Calculated values using measured k values COSMOS model
Overall temperature increase due to contact resistance between sidewall and closeout	C/C is expected to be 20% better based on surface roughness measurement. It is also softer which should improve the heat transfer.		0.5 $^{\circ}C$ aluminum/composite measured at SLAC; Calculate 1.4 $^{\circ}C$ at $h=1000W/m^2K$ , 14 $^{\circ}C$ at $h=100W/m^2K$ . Calculated values do not include benefit of fastener in transferring heat.
<b>STRENGTH<sup>5</sup></b>			
Launch axial load (N)	60	60	
Pull through test Insert / no insert (N)	645/191	1441/578	Average of 4 tests
<b>Safety Factor</b>	<b>10.8/3.2</b>	<b>24/9.6</b>	
Launch tangential load (N)	195	195	
Shear out tests Insert / no insert (N)	1290/436	1817/1443	Average of 4 - 90 $^{\circ}$ tests (worst case)
<b>Safety Factor</b>	<b>6.6/2.2</b>	<b>9.3/7.4</b>	
<b>COST</b>	\$102,600	\$	Production quantity totals
Per panel base cost	\$1350	\$	For flight quantities
Insert cost	+ (Additional \$)		C/C panels may be damaged by fasteners; inserts required in all holes.
Coating cost	+ (Additional \$)		C/C may require coating for particulate lockdown
<b>SCHEDULE</b>			
	12 weeks	8 weeks	ARO. All-Comp at the mercy of other vendors in meeting schedules

The P30 C-C sidewalls initially look better from both a thermal and cost standpoint. These two advantages do not outweigh the additional schedule constraint and the decreased mechanical strength when compared to the YS-90A/CE sidewalls. Moreover, because of the lower mechanical strength and particulate residue involving the carbon panels, additional cost would be incurred to coat the P30 C-C panels with Parylene for particulate lockdown and to bond metallic inserts into the sidewalls to improve pull out and shear out strengths. The TKR tower sidewalls were down-selected to be fabricated from YS-90A/CE.

<sup>4</sup>  $\Delta T$  calculations based on 9 heat inputs on a side, of 0.35 W each; layout from SLAC.

<sup>5</sup> Strength calculations based on COSMOS model, no clips on top but continuous attachment to grid.

## 5. Tracker Mechanical Design Concept

### 5.1 Tracker Tray Sandwich Structure Design Concept

The TKR tray sandwich structures are required to carry the SSD and TMCM payload into orbit. The trays must ensure that the payload survives the launch environment, as described in Section 3. There are currently five tray configurations. The standard tray configuration supports silicon payload on both sides, 3% of a RL of tungsten converter foil on one side, and two TMCM's. Figure 6 shows a rendering of the standard tray with its entire payload for reference. The second configuration is the standard tray without the tungsten converter foil. The SuperGLAST tray configuration supports silicon payload on both sides, and two TMCM's, as with the standard tray configuration, but here, the tungsten converter foil is increased to 18% of a RL. The top and bottom tray configurations have been designed to be structurally identical. The face sheet, closeout frame and core material are the same, however the payload is slightly different. The top tray is carrying silicon on one side, one TMCM, and 3% of a RL of tungsten converter foil. The bottom tray is also supporting silicon on one side, and one TMCM, however the converter foil is not included on the bottom tray.

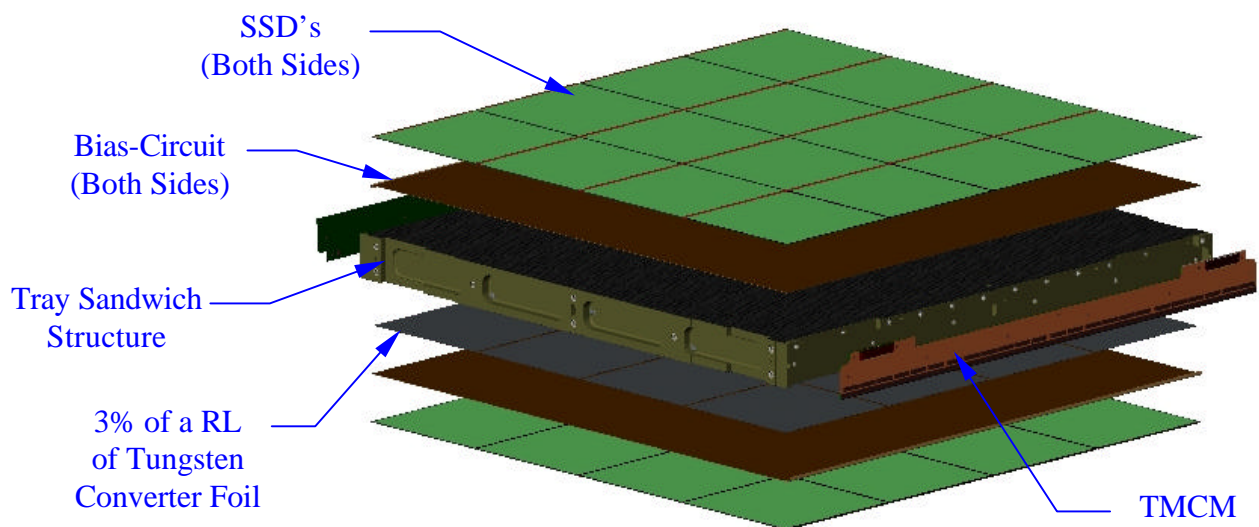


**Figure 6. Standard Tray Configuration with SSD's, TMCM's, 3% of a RL of Tungsten Converter Foil, and Bias-Circuit.**

#### 5.1.1 Standard Tray Configuration With/Without Converter Foil

*References: Drawings 102-TKR-12-3030, 102-TKR-13-3000*

The material selection is described in Section 4. Figure 7 shows a rendering of the standard tray mechanical components; the closeout frame, face sheets, and core are represented. The closeout frame is a bonded structure fabricated from four individual closeout walls. Figure 8 illustrates the MCM closeout wall. The MCM closeout wall supports the TMCM's during launch and is responsible for conducting the heat from the TMCM's to the thermal sidewalls. The thermal boss is identified in Figure 7. The structural wall completes the closeout frame on the

two remaining sides and provides a mechanical connection to the sidewalls. Figure 9 illustrates the structural closeout walls. Pockets are identified on the front of the structural closeout wall and the back of the MCM closeout wall. These pockets are included in the design to reduce the mass and minimize the amount of material in the gamma-ray path.

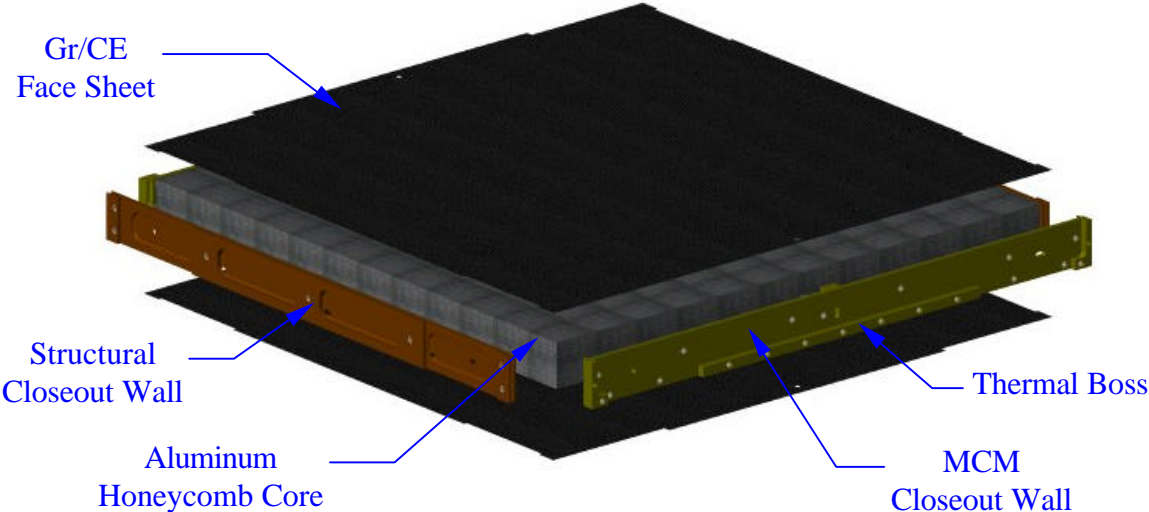


**Figure 7. Mechanical Components that make up the Standard Tray Configuration.**

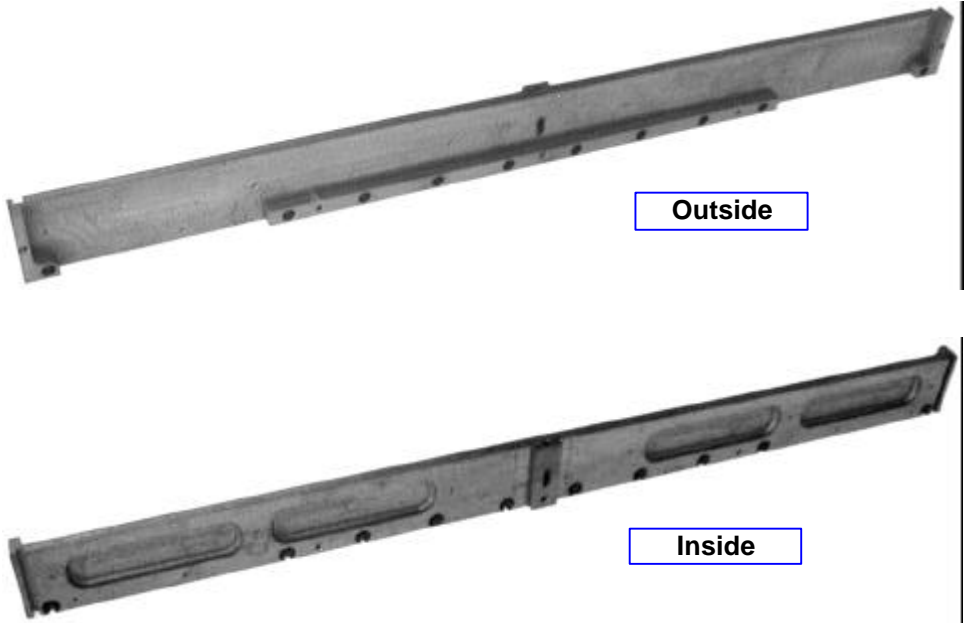


**Figure 8. Machined MCM Closeout Wall Prototype.**

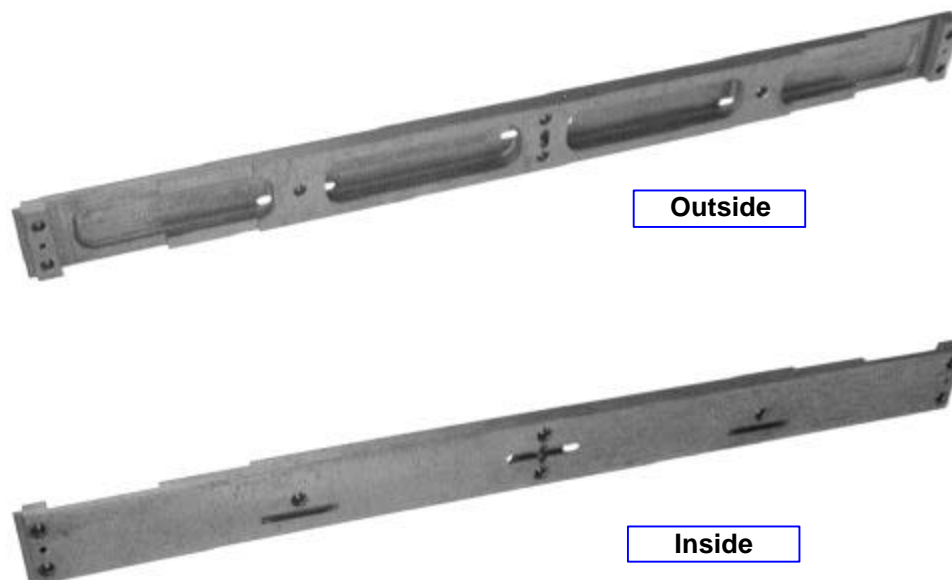


**Figure 9. Machined Structural Closeout Wall Prototype.**

The standard tray sandwich structure is constructed using unbalanced 4-ply composite face sheets. The term unbalanced used here refers to the layup being non-symmetric about the laminate neutral axis. This design choice was made to reduce the amount of material in the gamma-ray path. The 4-ply face sheets are oriented in the sandwich structure such that two face sheets are bonded to the core and balanced about the neutral axis of the sandwich structure. This type of construction has been used as primary structure by other satellite manufacturers on a number of satellite programs [Echostar III & IV, GE-3 & -4, Koreasat-3, to name a few projects]. The construction techniques are proven and composite vendors experienced with these construction techniques are being used to fabricate the prototype trays. Refer to HYTEC drawing 102-TKR-12-3030 (4-Ply Face Sheet) and 102-TKR-13-3000 (Mid Tray Assembly) for a more detailed understanding of the tray configuration as described above.

The face sheet and core selection was sized for minimum mass and ease of fabrication. For this reason, the core material used on the standard tray is the lightest commercially available that meets the stiffness requirements outlined in Section 3. The core material is aluminum, as described in Section 4, and perforated to provide a means of venting trapped gasses during launch.

#### *5.1.2 SuperGLAST Tray Configuration*

The SuperGLAST tray configuration supports a heavier payload. For this reason, the face sheets and core have been modified to provide more stiffness during launch, but the closeout frame is identical to that of the standard tray configuration. The 4-ply face sheets have been replaced with 6-ply quasi-isotropic face sheets, and the 1.0 lb/ft<sup>3</sup> core has been replaced by a 3.0 lb/ft<sup>3</sup> core, again, to provide greater stiffness. The combination of these changes allows the sandwich structure to meet the launch requirements.

### 5.1.3 Top/Bottom Tray Configuration

The top and bottom trays have been designed to be structurally identical, although inverted in the TKR tower assembly. Their orientation within the tower module is such that they are mirror images of one another. The closeout frame height has been increased by 6 mm to allow sufficient clearance for the tower-to-grid flexure mounts, as well as provide sufficient clearance for the tower lifting fixtures. This is illustrated in Figure 10.



**Figure 10. Top and Bottom Tray Sandwich Structure Configuration.**

In addition to modifying the closeout height, the sandwich thickness was reduced to  $\frac{3}{4}$  the standard tray core thickness. This modification was made, again, to allow for additional clearance for the tower-to-grid flexure mounts, as well as the tower lifting fixtures. This modification was acceptable because the reduced payload increased the fundamental frequency and decreased the dynamic response of the tray to the random vibration inputs. The face sheets and core material are the same as those used in the standard tray configuration, with the exception of some dimensional differences.

### 5.1.4 Tray Mechanical Performance

*Reference: HTN-102070-0005*

A considerable amount of finite element modeling and analysis has been performed to date to characterize the five trays to the launch and operating environment. This information is presented in a design report titled “GLAST Tracker Static and Dynamic Analysis”, HYTEC technical note HTN-102070-0005. A condensed version of the tray level mechanical analysis follows:

A major consideration in the design concepts selected for the tray construction was based on the need to protect the silicon from damage during launch. The silicon is at risk of damage if a tray and its payload were to collide with an adjacent tray during launch. The separation distance between trays is nominally 2mm, however the wire bond height uses 800  $\mu\text{m}$  of this. To avoid collision during launch, a design goal of 500 Hz fundamental frequency was identified as a satisfactory goal with an acceptable level of risk. This goal was derived with the assumption that an acceptable level of risk is measured by a 5% probability that one peak might exceed collision levels during the 60 second qualification level random vibration tests. This frequency requirement is initially very conservative because phasing information is ignored and internal damping is

assumed low ( $Q = 40$ ). The peak amplitudes will be reduced if the internal damping is increased. Also, the tray-to-tray phasing will reduce the level of risk as the trays move towards being in-phase. However, this frequency also assumes a fixed-base boundary condition in the tray analysis. In section 5.3.2, it will be shown that the fundamental frequency of the trays is reduced because of the compliant boundary condition, when mounted to the tower sidewalls. The effects are to be studied in the coming months.

Silicon payload attachment methods are currently under investigation. The adhesive used to attach the SSD's, epoxy vs. silicone, and the thickness of this adhesive are under development. Both variables impact the mechanical coupling of the silicon to the TKR trays. However, stiffness contributions from the silicon have been neglected up to this point. This also assumes that the relative displacement of the silicon to tray is negligible. Table 9 lists the calculated first mode frequencies of the five tray configurations. Two values are given, tray frequencies without any payload stiffness contributions (mass is only considered), and tray frequencies with stiffness contributions from the tungsten converter foil and bias-circuitry. It is clear that there will be significant stiffness contributions from the payload. Tray-to-tray collision is not considered to be of concern, based on this analysis.

**Table 9. First mode frequencies for the five tray configurations. Payload stiffness contributions are considered in the right-hand column.**

Tray Description	Frequencies (Hz)	
	Without Payload Stiffness Effects	With Payload Stiffness Effects
Top Tray	569	673
Standard Tray	584	711
SuperGLAST Tray	462	608
Standary Tray w/out Converters	718	764
Bottom Tray	767	788

A typical primary mode shape of all five tray configurations is shown in Figure 11. It is a drumhead mode with relative motion out of plane.

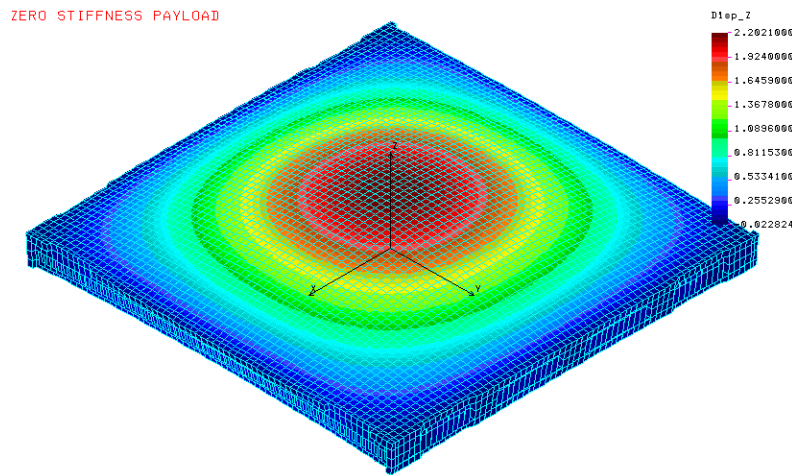


**Figure 11. Typical first mode shape of the five tray configurations.**

## 5.2 Tracker Tower Sidewalls

The TKR tower sidewalls have a dual-purpose role for the TKR tower. They provide about 80% of the tower stiffness and strength, in addition to removing heat generated by the TMCM's to the grid for distribution into the heat pipes and out to the radiators. To accommodate both aspects, a laminate ply-orientation was designed to provide the strength and stiffness characteristics necessary to meet the design requirements, while also providing good thermal conduction down the walls. A decision was made to use fabric material on the outside of the laminate and uni-directional tape in the center. The fabric provides strength and stiffness to carry loads and support fasteners, and the inner ply's are biased to enhance heat transfer. Section 6.1.2.2 describes the laminate geometry and thermal aspects of the sidewall layup. Mechanical coupon testing shows that the sidewalls have sufficient strength to support launch loads, without the use of metallic inserts. Sidewall prototypes have been ordered and will be tested at the tower level in the coming months.

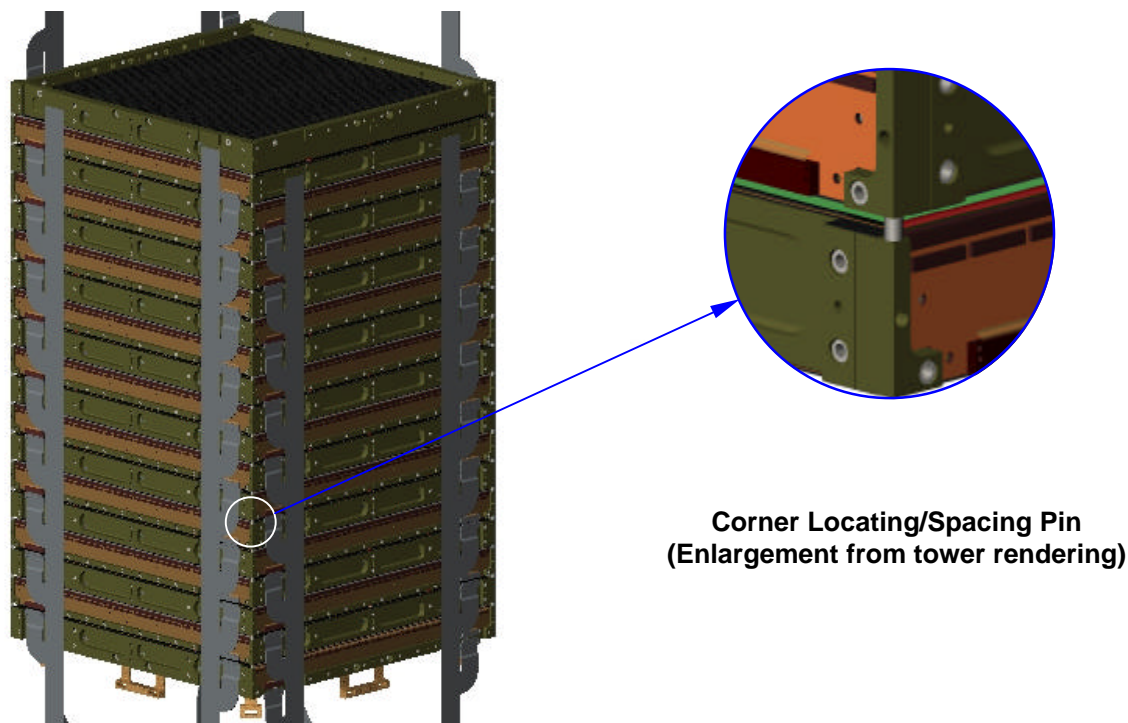
## 5.3 Stacked Tray Tracker Tower

### 5.3.1 Stacked Tray Design Concept

The stacked tray design concept is very simple in principle, but slightly more difficult in practice. The primary objective of this design concept is to simplify tower assembly and minimize the tower assembly time. The design philosophy used here is to build the TKR tower alignment precision into the mechanical components at the tray level. This will eliminate the need for elaborate tooling and fixturing to align the TKR trays during assembly, which would result in longer assembly times to complete the tower assembly.

In this scenario, TKR trays are fabricated with a high degree of precision at the component level and subsequently stacked on top of one another until all 19 trays are in position. A tower compression fixture will be used to compress and hold the stack while electronics cables are installed. The sidewalls will be installed at the last possible moment, without concern for alignment.

To accomplish this task, the precision will be built into the tray sandwich structures. This is done by critically locating the four corner post holes on each tray. With sufficient precision at this level, the trays can easily be stacked to meet the tower lateral alignment requirement of  $\pm 150$   $\mu\text{m}$ . The trays will be stacked using locating/spacing pins in each of the four corners, as shown in Figure 12.



**Corner Locating/Spacing Pin  
(Enlargement from tower rendering)**

**Figure 12. Illustration of the stacked tray design concept with corner locating/spacing pins shown.**

Once the stack is assembled, the tower will be secured using a tower compression tool. This will allow the stack to be worked on without the risk of toppling. Electronics cables can be secured without sidewalls interfering with assembly.

With the tower stacked and electronics in position, the tower sidewalls can be installed. Four unique sidewalls will be secured to the tower with counter-sunk fasteners. Countersunk holes in the sidewalls are necessary to ensure that the fasteners do not penetrate the 1.5mm tower-to-tower spacing. It is impossible to estimate the effect countersunk holes will have on the tower alignment, however it is believed that the net change to tower alignment will be minimal, and the tower alignment will meet design requirements. A critical step in the program plan is to build a tower and demonstrate that the alignment can be achieved using countersunk holes in the sidewall. Figure 13 illustrates the sidewall installation.

The TKR tower is now completed and ready for the flexure mount installation. This installation is done just prior to placing the tower on the grid to avoid damaging one of the flexures during assembly. Bottom tray flexure mounts are shown in Figure 14. The TKR tower is handled and positioned using a tower lifting fixture, as illustrated in Figure 15. This fixture will allow the tower to be easily integrated into the instrument package.

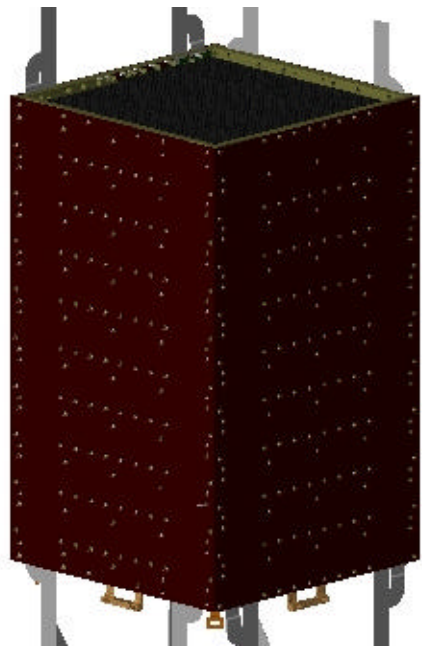


Figure 13. Illustration of the TKR tower with sidewalls installed.

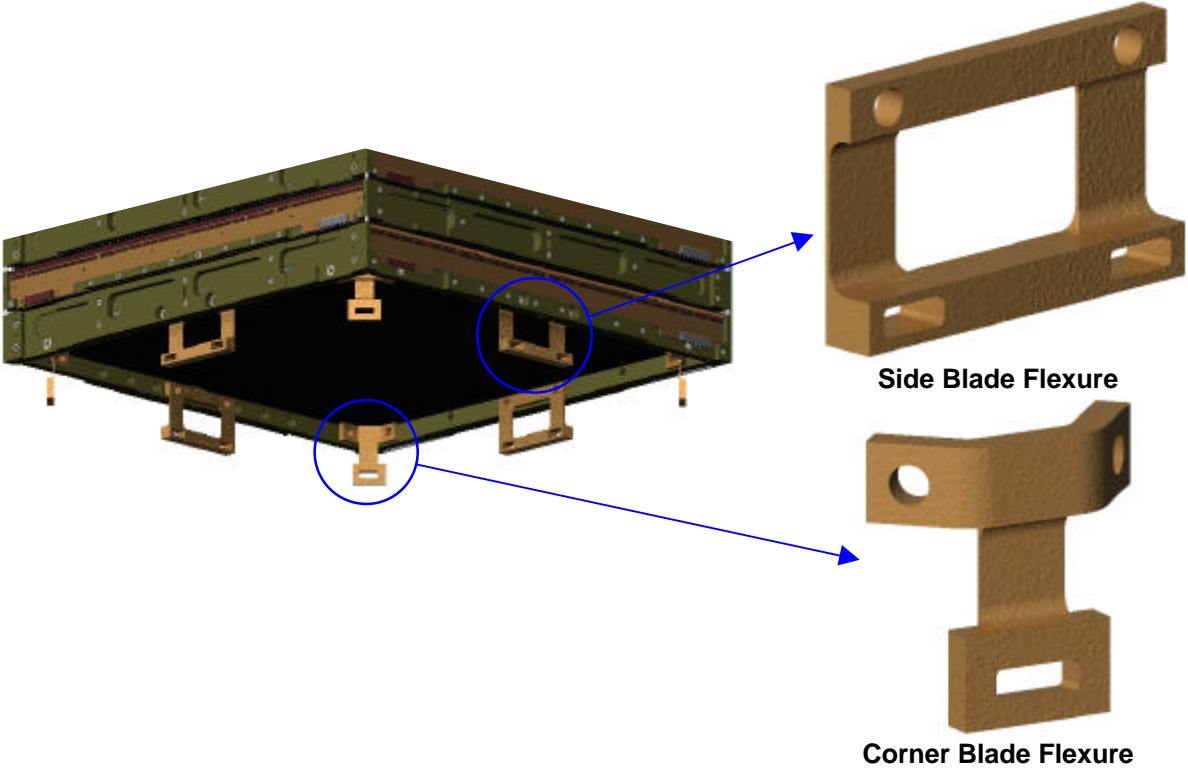
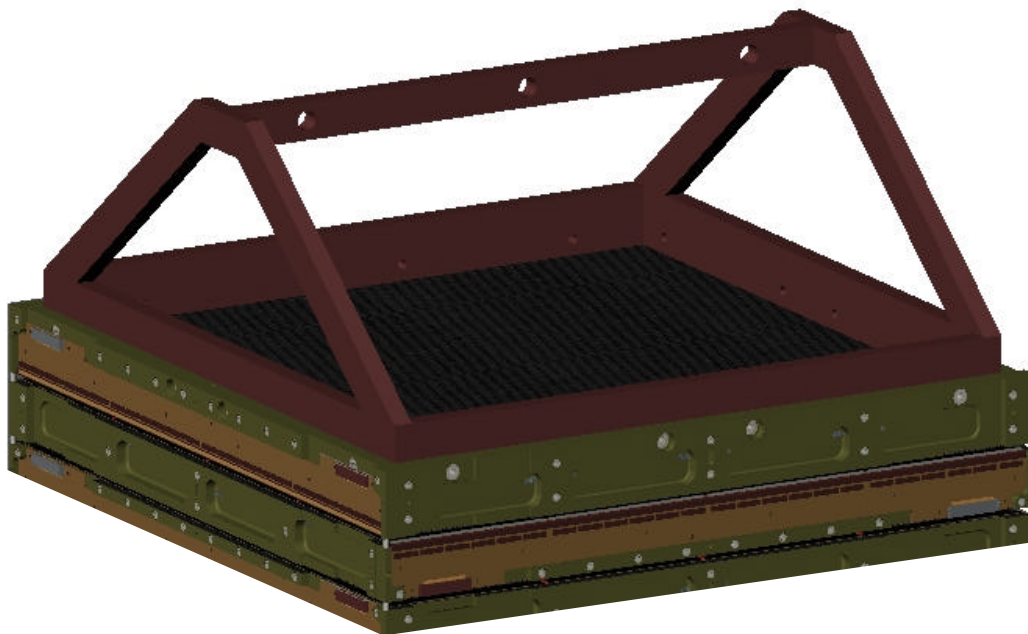


Figure 14. Bottom tray flexure mount configuration with two blade flexure types shown.



**Figure 15. TKR tower lifting fixture concept.**

### 5.3.2 Tower Mechanical Performance

*References: HTN-102070-0005*

A considerable amount of finite element modeling and analysis has been performed to date to characterize the TKR tower trays to the launch and operating environment. This information is presented in a design report titled “GLAST Tracker Static and Dynamic Analysis”, HYTEC technical note HTN-102070-0005. A consolidation of the tower level mechanical analysis follows.

Several key issues govern design choices for the TKR towers. The TKR tower-to-tower spacing is currently set at 1.5mm, which may be increased to 2.5mm. Given the 1.5 mm spacing, it is critical that the TKR towers have sufficient stiffness to prohibit the towers from colliding during launch. The towers must also have sufficient strength to prevent any type of mechanical failure in the tower mechanical components.

The TKR subsystem design group is currently responsible for all TKR components above the grid. With this assumption, the systems level response of the TKR towers falls under the SI systems design group. The TKR tower analysis assumes that the TKR tower is fixed to a rigid support at the bottom of the flexures. All analysis presented herein is calculated under this assumption.

Several elements can consume portions of the 1.5 mm tower-to-tower spacing. These include tower alignment, tower integration with the grid, static response, random vibration response, and thermal response. Each element will need to be assigned a portion of the 1.5 mm space for design purposes, however this has not been done to date. The breakdown, as assumed here, is defined in Table 10.

**Table 10. Projected breakdown of 1.5 mm tower-to-tower spacing, as used for TKR design purposes.**

Tower Alignment	300 μm
Tower Integration	200 μm
EMI Shielding	200 μm
Static Response	200 μm
Random Vibration Response*	400 μm
Thermal Response	200 μm
<b>Total</b>	<b>1500 μm</b>

\* RV allocation needs clarification

Tower alignment was discussed in section 5.3.1. Tower integration is the responsibility of the systems integration team. The static, dynamic and thermal response of the TKR tower is the responsibility of the TKR team up to the fixed base boundary. Of these elements, the random vibration values are the least known.

#### 5.3.2.1 Tower Frequencies

The TKR tower fundamental frequencies were calculated for two different tower support configurations. The two support configurations are the tower bottom tray fixed directly to a rigid support, and the bottom tray supported by the flexure mount configuration discussed earlier. Table 11 lists the first 20 modes and a description of the mode shape.

**Table 11. Detailed FEM tower modal frequencies.**

Mode	Description of Mode Shape	Bottom Tray Fixed Support (Hz)	Flexure Mount Support (Hz)
1,2	Cantilever bending mode from compliant support	363	125,130
3	Tower module vertical accordion mode	-	294
4	Tower module torsional mode	-	375
5,6	Tower module cantilever bending mode - Lateral	-	424,435
7-10	SuperGLAST tray drumhead mode	444 to 448	447 to 485
11	Top tray drumhead mode	527	534
12-20	Standard tray drumhead mode	542 to 554	553 to 555

From this analysis, it is clear that the flexure mount support configuration has a significant impact on the tower stiffness. This mounting configuration will be studied in more detail after PDR to ensure that the flexure mounts are not the cause of tower-to-tower collisions. Another detail that can be taken from this information is the reduction of the tray frequencies. This is a direct result in changing the rigid boundary conditions used in the tray FEM to a more compliant boundary condition, as with the TKR tower sidewall attachment.

#### 5.3.2.2 Tower Random Vibration Response

The tower module FEA included a series of studies to calculate the dynamic response of the tower when subjected to the qualification level random vibration input spectrum. The results are listed in Table 12.

**Table 12. RMS displacement response of the tower module due to the qualification level random vibration input spectrum at the support (Q=40).**

Direction	RMS Displacement ( $\mu\text{m}$ )	
	Base Support	Flexure Support
Vertical	220	204
Lateral	178	761

It is clear that the flexure support significantly impacts the dynamic response of the TKR tower. Some things to consider are: 1) tower phasing information is neglected, 2) a Q=40 is a conservative estimate and must be measured, 3) the excitation source is at the base of the tower, neglecting any attenuation from the softer grid bellow, 4) the thermal gasket material was neglected in this analysis. We will be addressing some of these issues in the coming months. The thermal gasket was recently included in the FEM and the RMS displacement dropped from 761 to 500  $\mu\text{m}$ . The TKR tower were included in the instrument model without the thermal gasket, and the RMS displacement was calculated to be 400  $\mu\text{m}$ . This would suggest that there is significant attenuation from the aluminum grid below the TKR tower. With all things considered, it is clear that the mounting configuration requires some additional work during the coming months.

#### 5.3.2.3 Tower Static Response

Static acceleration loads were studied at the tower module level. The two load cases included the liftoff & transonic, as well as the main engine cutoff (MECO); the load levels are defined in Section 3. Maximum displacements, stresses and fastener loads were calculated for each load case and for each support configuration. Table 13 lists the results of the static analysis.

**Table 13. Static response of the TKR tower module due to the applied acceleration conditions.**

Displacement, stress, or load description	Liftoff and Transonic		MECO	
	Base Support	Flexure Support	Base Support	Flexure Support
Maximum Displacement	12 $\mu\text{m}$	87 $\mu\text{m}$	14 $\mu\text{m}$	28 $\mu\text{m}$
Max Von Mises Stress	16.40 MPa	98.50 MPa	4.82 MPa	50.0 MPa
Max Axial Force	3.11 N	11.80 N	2.80 N	10.34 N
Max Shear Force	167.6 N	233.2 N	83.3 N	128.2 N

It is clear from this analysis that the TKR tower will support the static acceleration loads applied during launch. Displacement and load levels meet the design requirements outlined in Section 3 with an acceptable margin of safety. Static analysis will be refined after prototype testing, however continued efforts will be limited.

In addition to the tower level response, additional analysis was performed to measure the stress in the tray corner joints, and to measure the stress in the flexures due to thermal deformation of the grid. The corner joints are necessary in this design configuration because they transfer load in shear from one tower sidewall to the adjacent sidewalls. Removal of this feature would transfer this load by way of a peel stress between the face sheet and closeout frame. The face sheet would most likely be damaged as a result.

The grid will expand about 0.5 mm between each tower due to thermal changes, and the flexures will be required to adjust for half that distance. The maximum stress induced in the flexures was calculated to be about 0.39 GPa, when 0.25mm thermal growth and 0.25mm machining tolerances are considered. The yield strength of the flexure material, 6AL4V titanium alloy, is 1.10 GPa and the ultimate strength is 1.17 GPa. Given these values, there is an acceptable margin of safety to allow additional modifications to be made to the flexure design in an effort to increase the fundamental frequency of the TKR tower when supported on the flexures. This design aspect will be studied in detail over the coming months.

#### **5.4 Mechanical Interfaces for the TKR Tower Mechanical Components**

The TKR tower interfaces can be categorized as mechanical, thermal, electrical and environmental. Thermal interfaces are discussed in Sections 6.1 and 6.2. Electrical interfaces are beyond the scope of this development work and will not be discussed. Environmental interfaces are defined in the requirements, Section 3, and should be reviewed if necessary. This section defines only the mechanical interfaces for the TKR tower mechanical components. This includes the mechanical trays and the TKR towers. Mechanical interfaces can be either internal or external. Internal interfaces are defined as those components that interface with the TKR mechanical components, and fall under the TKR WBS. External interfaces are defined as those components that interface with the TKR mechanical components, but fall under any other WBS. The following mechanical interfaces are defined for the TKR mechanical components.

##### *5.4.1 Internal Interfaces*

Internal mechanical interfaces include the attachment of the SSD's, bias-circuits, & tungsten converter foils, as well as the attachment of TMCM's. A third internal interface would include the handling fixture used during SI integration. These interfaces are further along in their development because internal communication allows for quick and easy solutions.

The tungsten converter foils and bias-circuitry will be fixed to the sandwich panels using a rigid setting epoxy and a continuous bond joint. This will provide good strength during launch with the added benefit of increasing the sandwich panel stiffness to reduce the risk of tray-to-tray collisions. The SSD's will be bonded to the bias-circuits using a compliant silicone type adhesive. The silicone was selected to reduce the mechanical coupling between the trays and SSD's, which in-turn will reduce the thermally induced stress when the SI is subjected to survival level temperature drops. Analysis shows that this method of attachment significantly reduces the thermally induced stresses in the silicon.

The TMCM's will be mounted to the closeout frame using both a double-sided adhesive tape and a series of fasteners. The fasteners will be threaded directly into the C-C material. This decision was made after some coupon tests indicated that the strength of the C-C material to pullout loads exceeded 400 N and the load from the TMCM's was negligible.

Features used to lift the tower and support its mass have been included in the current design concepts. Actual lifting fixtures are in a preliminary state, however minimal development is expected. This issue will be resolved in the coming months. There is no technical reason to believe that the current solution will not be adequate. Figure 15 illustrates a lifting concept supported at eight points on the top tray.

#### 5.4.2 External Interfaces

In the current design, there is only one external mechanical interface for the TKR towers. This interface is the TKR-to-Grid interface. The TKR tower will be mounted on the aluminum Grid support structure. At this interface, there are both thermal and mechanical issues to be resolved. The physical interface has been defined as the plane(s) that separate the TKR tower from the grid. All TKR mounting hardware is considered to be the responsibility of the TKR WBS. All TKR analysis assumes a fixed base boundary condition at the base of the TKR tower.

Thermal issues that exist at this interface include both the heat transfer of thermal energy given off by the TMCM's and the CTE mismatch effects of the Composite TKR tower and the aluminum grid. To resolve the heat transfer issue, a Cho-Therm® gasket (or equivalent) is being considered to transfer the heat into the grid/heat pipes. Analysis indicates that the temperature increase across this boundary will be minimal, < 0.5°C. Mechanical issues will be studied through analysis and testing in the coming months to ensure adequate pressure can be achieved and maintained during launch.

The CTE mismatch issue is also under investigation. The current design concept is to mechanically isolate the TKR tower in-plane dimensions from the aluminum grid using a series of blade flexures mounted radially from the center of the TKR tower. Figure 14 shows the blade flexure configuration and the two flexure types. The flexures are arranged in a manner that secures the tower in all 6-DoF's, but allows in-plane expansion/contraction of the aluminum grid as the temperature changes. The thermal growth is expected to be as high as 0.5 mm (0.020"). A key issue that is currently being resolved is the effect these flexures have on the tower stiffness. The fundamental frequency drops from 363 Hz to 125 Hz, which increases the RMS displacement from 178 μm to 761 μm. The Cho-Therm® provides additional stiffness, increasing the fundamental frequency to 162 Hz, and decreases the RMS displacement to 495 μm.

The mechanical issues are being resolved with grid subsystem engineers. The approach has been agreed upon at this time, but the details of this interface have yet to be resolved. These issues will be resolved in the coming months.

## 6. Tracker Thermal Design Concept

### 6.1 Thermal Conduction

#### 6.1.1 Tracker Tray Sandwich Structure

*References: HTN-102070-0006, HTN-102050-0026*

##### 6.1.1.1 Design Concept

The TCMC boards are the main source of heat generation on the TKR towers. Each board produces about 0.35 watts of heat. The TCMC boards are mounted by conductive tape and fasteners on two sides of each GLAST TKR tray except for the top and bottom trays, which have only one face covered with silicon detectors thereby requiring only one TCMC board. The total number of TCMC's per TKR tower is 36. The total heat load generated by a tower is 12.6 watts.

The heat path for thermal heat leaving the TCMC boards is by conduction through the 3D C-C closeout walls of each TKR tray closeout frame and into the sidewalls via a thermal boss machined on the same sides of the frame as where the TCMC boards mount. Because the thermal path is through the C-C closeout frame, the thermal gradients of the frame become important. A thermal FEA was done on the closeout frames to determine what the thermal gradients looked like and how the frame geometry affects the thermal heat transfer from the TCMC boards to the sidewalls. The face sheets were also considered to see how much thermal temperature sharing was occurring across the trays since the heat load is on only two sides of a tray and each tray is connected to all four sidewalls.

##### 6.1.1.2 Face Sheet and Core

The thermal conduction through the face sheets was analyzed using a FEM with shell elements. Figure 16 shows the thermal gradients across the face sheets for a tower. The maximum thermal gradient for the face sheets is 1.0°C. The model does indicate that there is some thermal averaging occurring across the face sheets with the four sidewalls. However, the major percentage of heat from the TCMC boards is conducted out through the closeout frame walls.

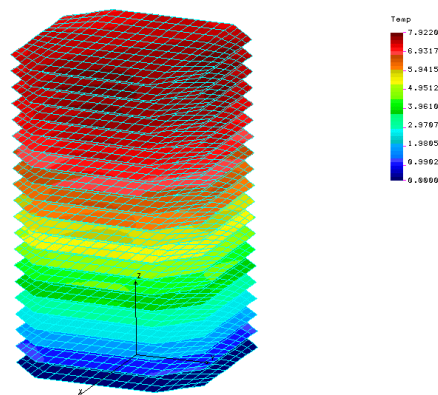


**Figure 16. Thermal Finite Element model of GLAST TKR Tower Face Sheets.**

The aluminum honeycomb core is bonded in between the two face sheets using a structural film adhesive FM-73. The thermal conductivity of the film adhesive is several factors lower than the face sheets or the core. The core was considered thermally isolated from the face sheets and the closeout frame walls because of its limited capacity to carry heat; heat transfer in the core was therefore not considered.

### 6.1.1.3 Closeout Frame

In the TKR tower there are two types of closeout frames, the standard tray frame and the bottom/top tray frame. Both closeout frames were analyzed using plane 2D FEM. Figure 17 shows the basic model boundary conditions for both models.

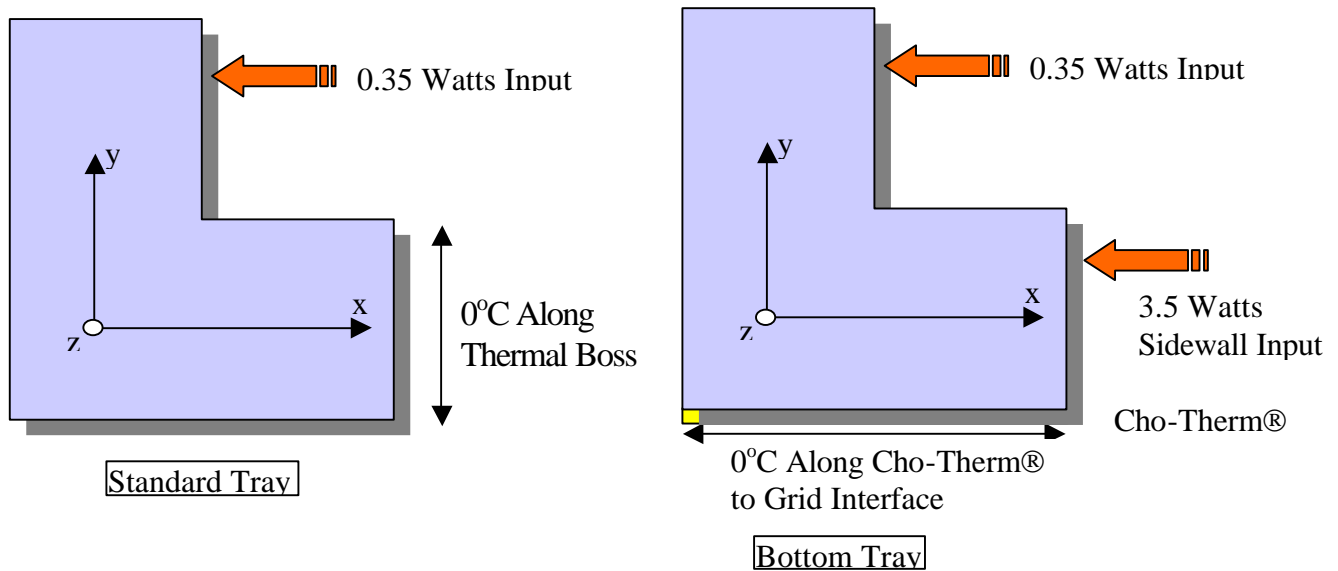


**Figure 17. Coordinate System and Boundary Conditions for Closeout Frame Thermal FE Models.**

Heat input of approximately 0.35 watts was placed along the TCMC board and closeout wall interface. A reference temperature of 0°C was set on the thermal boss of the standard tray closeout wall. The upper wall thickness of the closeout wall was varied from 5mm down to 1mm to see how the temperature profile varied with wall thickness.

In the case of the bottom tray, the heat transfer path is slightly different from the standard tray. A thermally conductive material is placed between the bottom tray and the grid. Heat from the tower must travel from the sidewalls through the bottom tray closeout frame and into the grid. In the case of the FEM, additional elements representing the Cho-Therm® gasket material were added along the bottom of the thermal boss and a thermal heat input was placed on the thermal boss from the sidewall heat conduction. The wall thickness for the bottom tray was kept constant at 3mm.

The models were then run for the temperature distribution through the closeout wall using the thermal conductivity values given for the 3D C-C closeout material. Table 14 lists the thermal conductivities for the material.

**Table 14. 3D C-C Material Thermal Conductivities.**

Conductivity Direction	Conductivity Value (W/m-K)
Kx	100
Ky	200

Table 15 shows the FE results for the carbon closeout frame. As can be seen in the results, the temperature gradients for the closeout frames are fractions of a degree indicating that since the majority of heat flow will follow the path of least thermal resistance, that pathway is through the closeout frame.

**Table 15. FE Results from Plane 2D Models.**

Standard Mid Tracker Tray				Bottom Tracker Tray	
Wall Thk = 5mm	Wall Thk = 2mm	Wall Thk = 1.5mm	Wall Thk = 1mm	Wall Thk = 3mm W/ Cho-Therm®	Wall Thk = 3mm W/O Cho-Therm®
0.045 °C	0.078 °C	0.096 °C	0.135 °C	0.34 °C	0.111 °C

### 6.1.2 Stacked Tray Tracker Tower

#### 6.1.2.1 Design Concept

The thermal design of the tower uses the four sidewalls to conduct the thermal energy from the tower electronics down the length of a tower to the bottom tray and on through to the instrument grid. In order to insure adequate thermal capacity, a complete thermal analysis was done on the sidewalls including material fiber selection, fiber ply orientation, and number of plies. To compare with the analytical results, a series of thermal property tests were done on the GFRC test samples. The properties determined from these tests were placed back in the thermal FEM of an entire tower to compare with analytical methods. Agreement was found to be very good between the two methods. K1100 fibers were used for the general analysis studies on fiber ply orientation because of the excellent thermal properties and the independence of fiber selection from ply orientation. Studies presented here were re-analyzed for actual YS-90 fibers to get temperature profiles for the actual sidewalls one fiber material selections were made.

#### 6.1.2.2 Sidewalls

In order to determine the thermal properties of the entire sidewall laminate, the individual lamina properties must be defined from the fiber and resin matrix. Since the sidewall laminate consists of multiple plies orientated at different angles, a rotation of thermal properties back to the original coordinate system must also be done for each ply. The plies can then be treated as multiple parallel paths similar to an electrical circuit with multiple parallel resistive paths to find the total thermal properties for the laminate.

##### 6.1.2.2.1 1D Thermal Sidewall Analysis: Lamina Ply Orientation

From Conley, the expressions for thermal conductivity of a lamina, in three orthogonal directions (one direction parallel to the fibers and other two directions perpendicular to the fibers) are given by:

$$k_{11} = V_f * k_{f11} + (1 - V_f) * k_m \quad (5)$$

$$k_{22} = k_m * \frac{k_{f22} * (1 + V_f) + k_m * V_m}{k_{f22} * V_m + k_m * (1 + V_f)} \quad (6)$$

$$k_{33} = k_{22} \quad (7)$$

Where,

- $k_{11}$  = lamina thermal conductivity, parallel to fibers.
- $k_{22}$  &  $k_{33}$  = lamina thermal conductivity, perpendicular to fibers and each other.
- $k_{f11}$  = fiber thermal conductivity, in the fiber longitudinal direction.
- $k_{f22}$  = fiber thermal conductivity, in the fiber transverse direction.
- $k_m$  = thermal conductivity of the resin matrix.
- $V_f$  = Volume fraction of fiber.
- $V_m$  = Volume fraction of matrix.

The orientation of the fibers in each lamina ply is then rotationally translated back to the original coordinate system. The rotation is done by multiplying the mathematical matrix of thermal values for the ply by the cosine or sine of the angle that the fibers in the ply are rotated from the original coordinate system. Figures 18 and 19 show how the thermal conductivity decreases or increases for the in-plane directions as the angle of fiber orientation increases from 0° to 90°. By referencing the thermal properties of every ply to one coordinate system, the values for each ply can then be combined to get the thermal properties for the entire sidewall laminate.

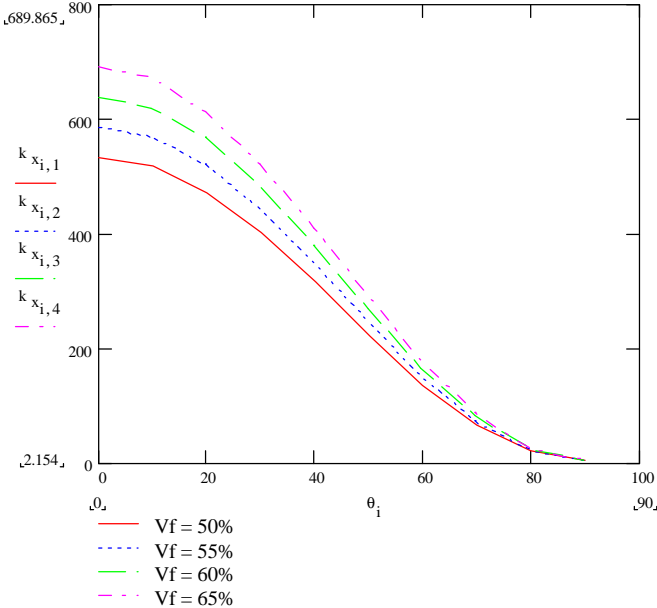


**Figure 18. Thermal Conductivity in Reference Coordinate System X-direction versus Ply Angle for a Single Lamina Ply and Varying Fiber Volume Fraction.**

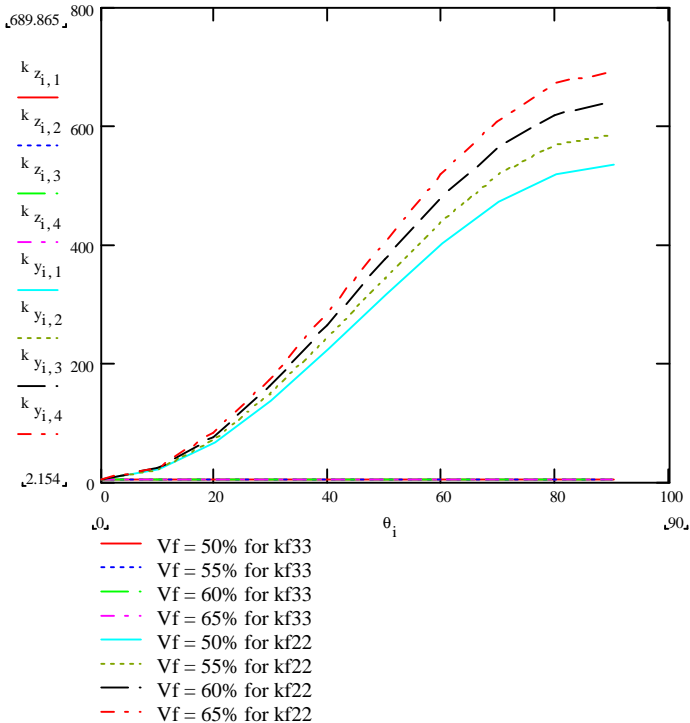


**Figure 19. Thermal Conductivity in Reference Coordinate System Y & Z-directions versus Ply Angle for a Single Lamina Ply and Varying Fiber Volume Fraction.**

6.1.2.2.2 2D Thermal Sidewall Analysis: Laminate Fiber/Ply Stack-up

Originally, several different ply angle combinations were studied in a FE model to determine the thermal conductivity effect. Figure 20 shows the average  $\Delta T$  from top to bottom of a sidewall as ply angles are changed.

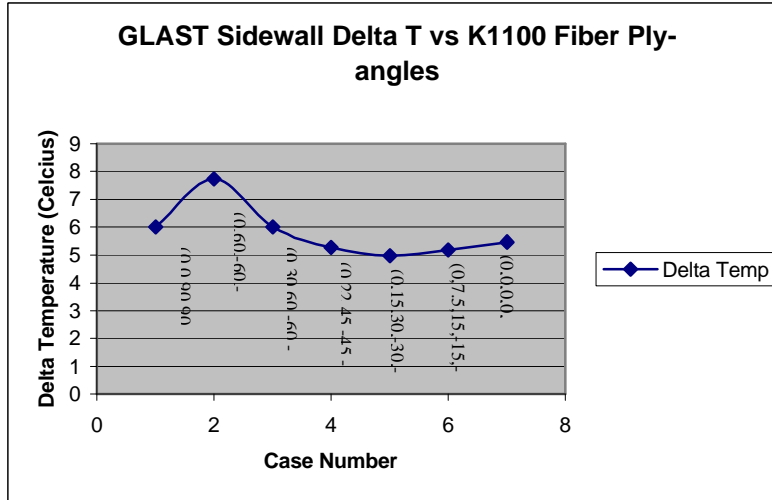


Figure 20. Average DT of K1100 Sidewall for Different Ply Angle Combinations.

Case four, although not the optimum was the most practical from a composites fabrication standpoint. The ply angles in case four are common for composite industry standards. The  $\Delta T$  for the sidewall in case four is also slightly better than case seven for a unidirectional composite panel. The difference is associated with better thermal cross distribution along the width of the panel, making the effective area of heat transfer much larger than with straight unidirectional plies.

The method used above for determining ply-angle orientation for the sidewall was very cumbersome and quite time consuming. To get a better distribution of how  $\Delta T$  varies with ply-angle orientation, a program was written that would automatically vary ply-angles in a FE model and plot the resulting  $\Delta T$  as a surface map. Figure 21 shows one of the surface plots generated for a K1100 fiber GFRP sidewall.

The surface plot has the same characteristic shape as Figure 20, but it easily shows more of the contour of the trough that forms around a ply-angle of 15 degrees and the expected peak for both plies having their orientation normal to the direction of thermal conduction in the panel. The surface plot was generated by first considering a six-ply laminate since that is the minimum number of plies needed to form a quasi-isotropic composite. Since the six-ply laminate is symmetric, only three ply-angles need to be specified. One of the plies is always orientated in the  $0^\circ$  ply direction, leaving the other two ply-angles ( $\alpha$  &  $\beta$ ) to be specified. The other two plies are defined from  $0^\circ$  to  $90^\circ$  by setting one ply-angle ( $\alpha$ ) and then running multiple cases with the other ply-angle ( $\beta$ ) being incremented from  $0^\circ$  to  $90^\circ$ .

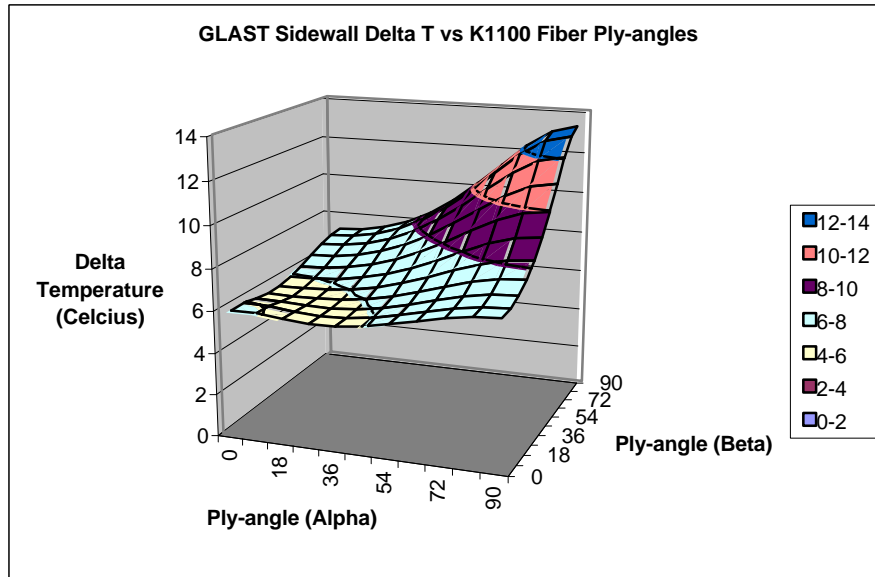


Figure 21. Sidewall Delta T versus K1100 Fiber Ply-angles.

Multiple surface plots were run with varying thermal conductivities for the different fiber possibilities. In addition to K1100 fibers, P30 and YS-90A fibers were studied. 3D FE sidewall analysis for the tower was done next to define thermal sharing between the four sidewalls.

#### 6.1.2.2.3 3D Thermal Sidewall Analysis: Tracker Tower

Thermal load sharing will occur between sidewall panels for each TKR tower. This is due to the large number of thermal pathways between sidewalls in the tray closeouts and face sheets. A brief FEA was done to determine how much thermal load sharing would occur in the GLAST TKR towers. Figure 22 shows the thermal gradients across four sidewalls connected at the corners.

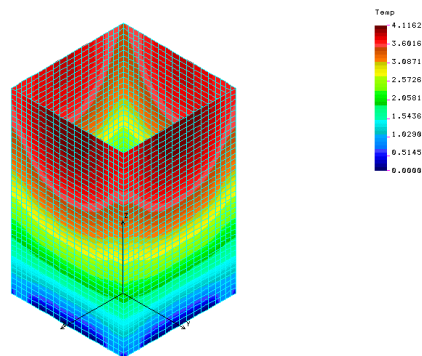
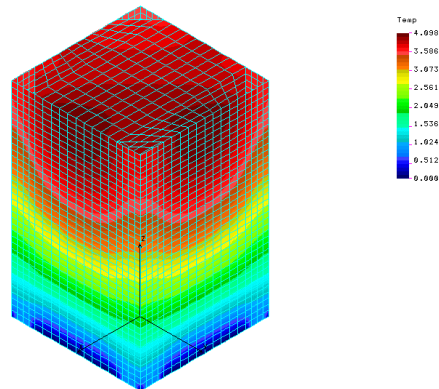


Figure 22. K1100 fibers, ply angle sequence: (0, +/-22.5, +/-45|symmetric).

Since the sidewalls are actually connected to the tray closeouts in the corners and not to each other, any redistribution of thermal load will occur through the tray closeouts. Selection of material for the closeouts will determine how much thermal load is transferred between the

sidewalls. Original FE models were developed w/o closeout frames for simplicity of the models and lack of development of the closeout frame.

The thermal gradients are relatively even around the four sidewalls. The maximum gradient from the top of the sidewalls to the bottom is 4.11°C. The model was revised to include the face sheet material between the four sidewalls. Figure 23 shows the resulting thermal gradients.



**Figure 23. K1100 fibers, ply angle sequence: (0, +/-22.5, +/-45|symmetric).**

With YSH50/RS-3 face sheet material included in the FEM, the maximum thermal gradient changed to 4.09°C. The thermal gradient changed by 0.02°C indicating a minimal redistribution of thermal load through the face sheets. This is probably due to the high thermal conductivity of the K1100 fibers in the sidewalls versus the minimal cross sectional area of the face sheets, which are 152µm to 229µm thick depending on the type of tray.

### 6.1.3 Tracker Tower Interfaces

#### 6.1.3.1 Internal Interfaces

Thermal conduction through internal interfaces in the tower will be limited to pressure contacts between the subcomponents and parts that make up the tower. This is a critical issue because of the ambiguity involved with defining heat transfer across a pressure contact. One of the more critical pressure contacts is the one between the sidewalls and the thermal bosses on the closeout frames.

Pressure contact tests were done between a sample of closeout frame material and sidewall material. The test consisted of taking pressure sensitive tape and sandwiching it between the two pieces. The pieces were then fastened together using the actual fasteners that were selected for attaching the sidewalls to the tower trays. The tape once stressed is then removed and sent to a lab where they determine the limits of pressure produced. Table 16 shows the results from the tests.

**Table 16. Results of Pressure Contact Tests for Sidewalls to Closeout Frames.**

P30 Carbon-Carbon		YS-90A	
Avg. Load (Lbf)	22.8	Load (Lbf)	36.2
Avg. Pressure (PSI)	52.9	Avg. Pressure (PSI)	55.8
Surface Roughness (µm)	10 to -10	Surface Roughness (µm)	12 to -12

The maximum load produced was 98.2 lbf near the fasteners, and it quickly drops off, as the distance from the fasteners increases. Average load for the thermal boss was right around 36.2 lbf. Estimates for thermal resistance are around 0.5°C across each contact boundary condition.

#### 6.1.3.2 External Interfaces

Thermal conduction through the external interface for the tower is located at the interface between the bottom tray and the instrument grid. A small layer of Cho-Therm® material is being considered at the base of each tower to increase the thermal conduction across this interface. Thermal conduction for the selected type of Cho-Therm® is 6.0 W/m-K. To ensure good thermal contact across the Cho-Therm®, the tower will compress the thermal layer when the flexures are bolted into place on the instrument grid.

In addition, a thermal path exists through each set of flexures at the base of each tower. The flexures are made from Titanium Ti-6Al-4V (Grade 5) STA. The poor thermal conductivity and the thin cross sectional area of the flexures prevent the necessary heat transfer from the tower to the grid. The Cho-Therm® at the base of each tower provides the main heat path out of each TKR towers.

## 6.2 Coefficient of Thermal Expansion

*References: HTN-102050-0015, -0018, & -0026*

### 6.2.1 Tracker Tray Sandwich Structure

#### 6.2.1.1 Design Concept

The CTE for the TKR trays was of significant importance due to the direct effect the tray structure would have on the detectors. Initially, the first SBIR and BTEM trays had aluminum tray closeout frames with aluminum honeycomb cores and Gr/CE face sheets. Thermal cycling of the trays demonstrated CTE mismatch issues in the SSD payload. Further tests were done to isolate the payload from the trays, but there are still CTE mismatch issues between the composite sidewalls and the original trays. An all-composite tray structure was investigated for this reason.

This all-composite tray structure proved to be very effective in reducing CTE mismatch issues. However, the reduction of CTE comes with a cost. The tray structure was three times more expensive. Further investigation came back with a reasonably priced composite closeout frame and face sheets. The core was kept as aluminum honeycomb since CTE issues did not center on the core.

### 6.2.1.2 Face sheets and Core

The face sheets had to be composite to minimize the amount of thermal stress the face sheets place on the silicon detectors due to thermal expansion. High thermal stresses were still being produced by the conversion material in the SSD layer; therefore, the composite face sheets also served to reduce the amount of thermal stress in the payload by limiting the amount of growth the converters could do when cycled from 50°C to -30°C. With the face sheets made from composite materials, concern was placed on using anything other than a composite closeout frame with similar CTE properties due to the bonded joint between the face sheets and the closeout frame. A composite closeout frame also addresses other interface issues where CTE mismatch would be of concern.

### 6.2.1.3 Closeout Frame

The closeout frame has interfaces with the composite sidewalls and the composite face sheets. Either CTE mismatch with the face sheets or the sidewalls could lead to fabrication or alignment problems. Face sheet de-bonding and high fastener stresses are of concern when the sidewalls expand or contract at a rate that is different than the closeout frames assembled in a tower. The alignment of the tower could also be affected with CTE mismatch between the sidewalls and the stacked trays. A great deal of time was spent considering the alignment of detectors with the CTE of the sidewalls. This information applies to the closeout frames as well and will be deferred to the sidewall section for further discussion.

## 6.2.2 *Stacked Tray Tracker Tower*

### 6.2.2.1 Sidewalls

For thermal loads, a material's thermal expansion governs alignment, geometric stability and thermally induced stresses. Higher CTE materials will experience greater deformations for a given temperature change. As tray alignment and overall geometric stability are a pre-requisite for the TKR tower design, low-CTE materials are preferable. Thermal stresses for components and/or fasteners may also be an issue if miss-matched CTE materials are used.

#### 6.2.2.1.1 Tracker tray alignment issues

Tray (detector) alignment is especially critical for the GLAST TKR. Thermal loading of the TKR towers will vary from the center of the tracker to the outer walls. We predict that the sidewalls will dominate tower deformations under thermal loading. Figure 24 shows a potential deformation mode for a single tower under a side-to-side temperature differential. One can reasonably assume that such a differential is linearly distributed. For an isotropic material, the curvature of the tower sidewalls is given by

$$\mathbf{k} = -\frac{\mathbf{a}\Delta T}{h} \quad (3)$$

where  $h$  is the tower width in the  $x$ -direction. Small angle approximation then gives the tower top rotation  $\mathbf{q} = \mathbf{k}L$  where  $L$  is the tower height. For point P, displacements in the  $x$ - and  $z$ -direction are  $-\frac{1}{2}\mathbf{q}L$  and  $\mathbf{a}\Delta TL$ , respectively. Point Q will move an additional  $\frac{1}{2}\mathbf{a}\Delta Th$  in the  $x$ -direction<sup>†</sup>.

---

<sup>†</sup> We consider only the horizontal displacement of point Q. Assuming  $T = 0$  at  $x = h$ , point Q has negligible vertical displacement. For composites, horizontal displacements of Q depend upon the material's  $x$ -direction CTE.

A summary of predicted displacements for the two indicated points on the tower is given in Table 17.

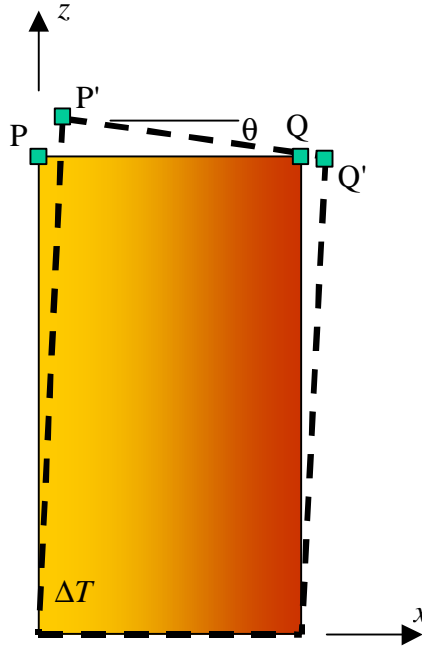


Figure 24. Deformed shape of tower under side-to-side temperature differential.

Table 17. Tracker tower top displacements for side-to-side temperature differential.

		DT = 2°C [x=0 ? T=2; x=h ? T=0]			DT = 5°C [x=0 ? T=5; x=h ? T=0]		
Material	CTE (ppm/°C)	P' <sub>x</sub> (mm)	P' <sub>z</sub> (mm)	Q' <sub>x</sub> (mm)	P' <sub>x</sub> (mm)	P' <sub>z</sub> (mm)	Q' <sub>x</sub> (mm)
Aluminum	23.6	23.1	29.3	32.4	57.7	73.2	80.9
Beryllium	11.3	11.1	14.0	15.5	27.6	35.0	38.7
Gr-CE Composite	z: -1.5 x: -0.5	-1.5	-1.9	-1.8	-3.7	-4.7	-4.4
CC Composite	z: -1.5 x: -1.2	-1.5	-1.9	-2.2	-3.7	-4.7	-5.5

Finite element analyses were also conducted to verify that the sidewalls dominate the deformation under thermal loads. Displacement results for aluminum sidewalls and tray closeouts, under a side-to-side temperature differential of 2°C.

### 6.2.2.1.2 CTE material mismatch

CTE mismatches in adjacent materials will induce stress due to unequal expansion (and/or contraction) of the materials under temperature changes. Therefore, matching CTE values (or minimizing CTE mismatch) for the tray closeouts<sup>†</sup> and sidewall materials should be considered. The current design for the tray closeout incorporates small spacer posts, bonded into each of the four corners<sup>‡</sup>. Additionally, small fasteners will be used to attach the sidewalls to each TKR tray. Figure 25 shows a corner of a typical tray closeout.

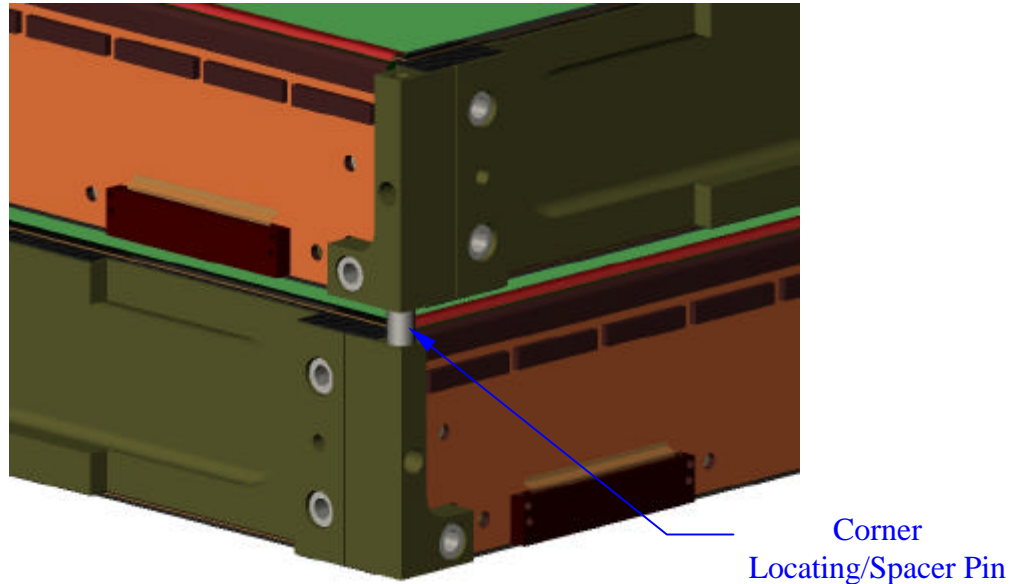


**Figure 25. Spacer post and fastener locations at corner of typical tray closeout.**

The closeout corner spacer post is restricted in size by spatial constraints of the TKR. Its dimensions are approximately 3.0-3.5mm diameter. If CTE mismatches exist between the closeout and sidewall materials, then each corner post must counter forces imposed by two sidewalls as the tower undergoes a temperature change from the assembly temperature.

We assume that there are a sufficient number of fasteners along the length of the tower to consider a continuous sidewall-to-closeout connection. For a conservative first-order analysis, we assume that the sidewalls act as axial (*Z*-direction) members. The average internal force, *P*, due to a temperature change in two continuously connected materials is given by

$$P = (\mathbf{a}_S - \mathbf{a}_C)\Delta T \frac{A_S E_S A_C E_C}{A_S E_S + A_C E_C} \quad (4)$$

where *S* and *C* refer to the sidewall and closeout, respectively. Stresses in the corner posts are determined in the usual manner. Table 18 shows resultant forces and stresses for the corner post for CTE-mismatched materials under a modest  $\pm 20^\circ\text{C}$  temperature change. Tests have shown

<sup>†</sup> Tray closeouts are the frames which surround each tray, providing support for the tracker detectors, conversion layers and other hardware.

<sup>‡</sup> Machined spacer posts may be replaced by (captured) spacer blocks.

that the compressive strength of 2D C-C composites ranges from 63 to 75 MPa depending on fiber orientation. Therefore, C-C closeouts would probably not work with aluminum or beryllium sidewalls.

**Table 18. From assembly  $DT = \pm 20^{\circ}\text{C}$  – resultant forces and corner post stress for CTE mismatch in sidewall and closeout materials.**

Sidewall Material	Closeout Material	Resultant Internal Force [N]	Corner post stress [MPa]
Aluminum	Beryllium	877	71.6
Aluminum	Carbon composite	1435	117.1
Beryllium	Aluminum	208	17.0
Beryllium	Carbon composite	775	63.3
Carbon composite	Aluminum	424	34.6
Carbon composite	Beryllium	975	79.6

For design purposes, we should assume conservatively that the internal force P will be developed fully in shear at the outermost fasteners connecting the sidewalls to the closeouts (i.e., those at the top and bottom of the tower). Spatial constraints require that the screws be limited in size to approximately 1-2.5mm in diameter. The loads shown in Table 18 indicate that substantial local stresses could be developed at the fastener locations. Additionally, if we assume a conservative static friction value of 1.0, we can see that the required normal loads to resist slippage could be excessive.

## 7. Tracker Fabrication and Assembly

*References: Drawing 102-TKR-13-6010*

### 7.1 Sandwich Tray Construction

Construction of the TKR trays begins with a simple multipurpose tool. The bonding fixture is made from isotropic statically pressed graphite, which keeps CTE differences to a minimum, and the material is considered very stable both thermally and structurally. The graphite-bonding tool was developed with input from composite vendors and an initial prototype. The bonding tool serves as a reference to control orientation of the four closeout frame walls to establish parallelism and perpendicularity of the trays. The bonding tool also allows for the bonding of the sandwich structure of the trays without removal of the closeout frame; thus, ensuring repeatability in the tray fabrication process.

A brief description of the assembly process is given here. A more detailed description of the assembly process can be found in HYTEC drawing # 102-TKR-13-6010. The assembly process starts with locating the graphite tool on a flat surface. The four closeout walls with fastener inserts already in place are aligned against the four inner sides of the tool and attached via several small finger screws (Step A.). Adhesive is added to the mortise and tenon joints before the walls are fully located inside the assembly tool (Step B.). The closeout frame is then held at 80°C for an hour to cure the adhesive. After cooling the entire assembly, the bottom face sheet is placed on the flat surface underneath the closeout frame and located using two small alignment pins that fit in the two bosses on the inner side of each TCM closeout wall (Step C.). Structurally backed film adhesive is added around the upper and lower edges of the closeout frame to attach the face sheets to the closeout frame. The honeycomb core, with reticulated film adhesive, is placed into the middle of the frame and the top face sheet is then placed on top of the core and closeout frame to complete the tray (Steps D. & E.). The whole assembly is then cured at 120°C for 1.5 hours. Figures 26 and 27 show the basic steps for tray assembly.

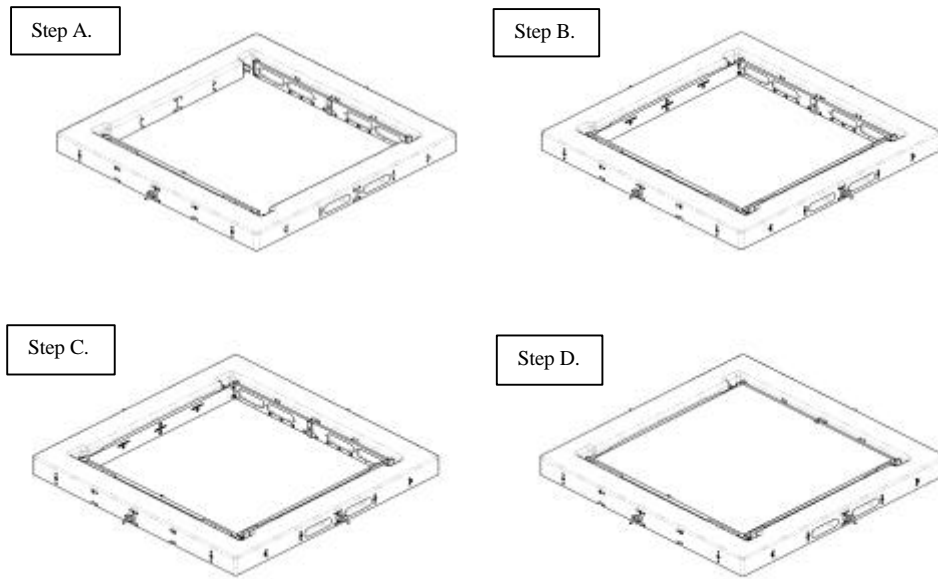


**Figure 26. Steps A. through D. for Tray Assembly.**

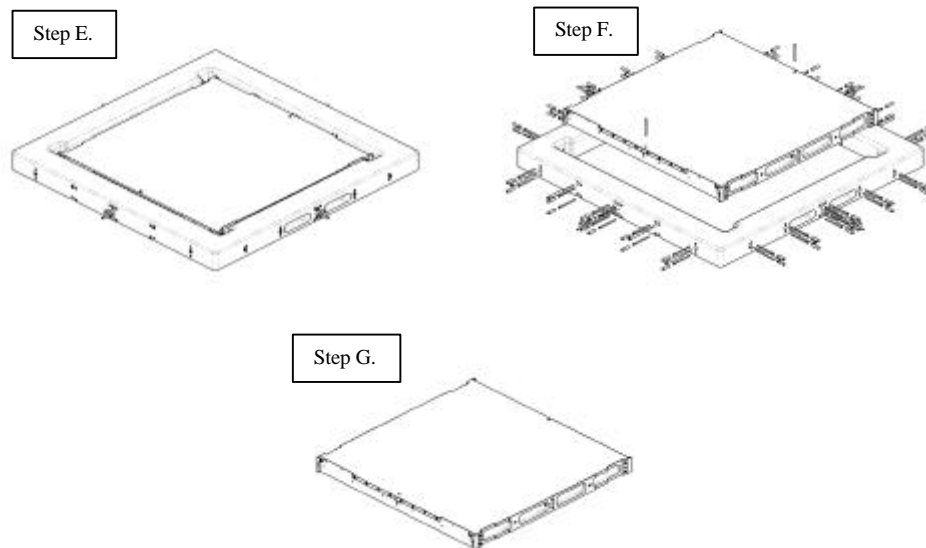


**Figure 27. Steps E. through G. for Tray Assembly.**

Upon cooling of the assembly from the second curing cycle, the finished tray is removed from the graphite tool (Step F.), and the finished tray is ready for final machining of the tray pin/locating holes in the four corners of the tray (Step G.). The location of the holes relative to each tray is an extremely important step because it defines the tray-to-tray alignment, as the towers are assembled. The hole pattern must be very repeatable from tray to tray with minimal

misalignment in hole patterns from top to bottom of each tray. Once the final machining is complete, the tray is ready for the assembly of the payload and detectors.

## **7.2 Tracker Stacked Tray Tower Assembly Concept**

The concept for aligning and stacking trays uses no external alignment tooling. Alignment is instead controlled by pinning the trays together in the four corners with spacers placed between trays to set the tray-to-tray spacing. This method of tower assembly defines the tower alignment using the tray as the building block. In order to achieve this alignment, the machine tolerances of the closeout frame have to be controlled uniformly from tray to tray. The tolerances on the tray closeout frame although small are within acceptable limits for machining. The close tolerances required to ensuring proper fit between trays are controlled by the graphite assembly tooling.

The assembly of a tower starts with bonding the spacer blocks into the bottom side of all four corners of each tray with the exception of the bottom tray. The trays are then stacked according to order: 1 bottom tray, 2 standard tray without converters, 4 Super GLAST trays, 11 standard trays with converters, and 1 top tray for a total of 19 trays. The trays are rotated between  $0^\circ$  and  $90^\circ$  as they are stacked up. The entire stack is then compressed using a compression fixture. This allows the electronics cabling to be installed without the sidewalls interfering. The sidewalls are then installed on all four sides using countersunk fasteners. The torque pattern used for sidewall fasteners will start at the bottom tray and work upward. Torque requirements for the sidewall fasteners are 80 cN-mm. Once all the fasteners are in place, the compression fixture is then removed. No additional alignment is required, and if further maintenance is required, the tower alignment does not need to be re-established by the removal of two opposing sidewalls.

## 8. Mechanical Structure Prototype Testing

The TKR engineering development approach was re-directed to support a series of coupon level and prototype tests. Coupon level testing was performed to validate material properties and various design concepts. Prototype testing will be performed at both the tray level and tower level to validate and update FEA as well as various design concepts. The following section outlines both the coupon level and prototype level testing performed to date.

### 8.1 Component Level Coupon Testing

A series of coupon tests were performed to validate material properties and various design concepts. These tests measured the material properties of the 3D C-C closeouts, face sheets, and sidewalls, in addition to measuring a number of design concepts.

#### 8.1.1 3D C-C Closeout Coupon Testing

Previous prototype testing used a 3D C-C material that was recycled from aircraft brake shoe material. Current prototyping is using a virgin form of the recycled brake shoe C-C material, which has undergone modifications to the material processing. For this reason, material property testing was performed to ensure that the 3D C-C material is equivalent to that used in previous prototypes. Tensile strength and elastic modulus measurements showed that tensile properties are equivalent. Flexural property measurements revealed a decrease in strength. This reduction is a result of increased material porosity, but is being improved by including additional resin re-impregnation steps. Thermal conductivity properties were measured and verified that the material is more porous than previous material samples. The conductivity values were lower by about 40%. The impact on the tower temperature drop, however, is negligible. Results are tabulated in Table 19.

**Table 19. Results of material property testing for the 3D C-C closeout material.**

	3D C-C	
	Recycled	New
<b>Strength/Modulus</b>		
In-Plane Tensile Strength (ksi)	11.9	11.4
Thru-Thickness Tensile Strength (ksi)	1.89	1.63
In-Plane Tensile Modulus (Msi)	5.3	6.1
Flexural Strength (ksi)	18.1	8.5
<b>Thermal Conductivity</b>		
In-Plane	204	135
Thru-Thickness	130	66

Strength tests were performed to validate design choices and concepts. Fastener/insert pullout and shearout testing was performed to verify that fastener/insert size and locations in the closeout frame are satisfactory. The results indicate that the strength of the material is sufficiently high to support the launch loads. Table 20 lists the results of these tests. M1.6, M2.5, and M3.5 fasteners/inserts were measured. The results of the M1.6 pullout tests were so positive that inserts for these fasteners were removed from the closeout frame design. The M1.6 fasteners

secure the TCM's to the closeout frame MCM walls, and the fasteners are now threaded directly into the C-C closeout material.

**Table 20. Measured shearout and pullout values for the closeout wall coupon testing.**

Test Description	Measured Values (N)
<b>Fastener Pullout</b>	
M1.6 Fastener in C-C Closeout	450
M2.5 Fastener in C-C Closeout	976
M2.5 Fastener in Al Insert	2160
<b>Fastener Shearout</b>	
M1.6 Fastener in C-C Closeout	Not Measured
M2.5 Fastener in C-C Closeout	1273
M2.5 Fastener in Al Insert	1550

In addition to the above tests, additional joint testing was done to validate and quantify the strength of the mortise and tenon joint proposed for the closeout frame. The results of these tests showed that the closeout frame could be bonded and handled as a stand-alone component and did not require the support of the face sheets. This was important to allow the closeout frame to be coated prior to assembly of the tray sandwich structure, if deemed necessary.

#### *8.1.2 Tray Sandwich Structure Face Sheets*

Coupon testing was planned to measure the material properties of the tray sandwich structure face sheets. However, sufficient historical data was available to justify forgoing this material property validation. As a result, witness coupons were taken from the prototype material and used to measure the elastic modulus of both the 4-ply face sheets and the 6-ply face sheets. The results for the 6-ply face sheet material were satisfactory, however the results for the 4-ply face sheet material were low.

Laminate theory predicts that the elastic modulus of both laminates would be 14.8 Msi. The 6-ply face sheet measured an average elastic modulus of 13.7 Msi. The 4-ply face sheet measured an average elastic modulus of 11.4 Msi. These results are presented in Table 21. These values are low, however they were included in the FEM to predict the effects on tray stiffness. The loss in stiffness was not significant. The fundamental frequency of the tray with this loss in material property is 584 Hz, as listed in Section 5.1.4. The tray sandwich structures are expected to survive the launch environment without incidence.

**Table 21. Predicted vs Measured material property values for the 4-ply and 6-ply face sheet laminates.**

GLAST Tracker Tray Face Sheets													
4-Ply							6-Ply						
Sample #	Predicted			Measured			Sample #	Predicted			Measured		
102-TKR-12-3030-1	Thk (in.)	FV (%)	E (Msi)	Thk (in.)	FV (%)	E (Msi)	102-TKR-12-3030-5	Thk (in.)	FV (%)	E (Msi)	Thk (in.)	FV (%)	E (Msi)
1	-	-	-	0.007	58	9.9	1	-	-	-	0.008	59	15.8
2	-	-	-	0.006	58	13.0	2	-	-	-	0.010	59	12.4
3	-	-	-	0.006	58	10.5	3	-	-	-	0.010	59	12.9
Avg. Total	0.006	60	14.8	0.006	58	11.1	Avg. Total	0.009	60	14.8	0.009	59	13.7
102-TKR-12-3030-3	Thk (in.)	FV (%)	E (Msi)	Thk (in.)	FV (%)	E (Msi)	102-TKR-12-3030-7	Thk (in.)	FV (%)	E (Msi)	Thk (in.)	FV (%)	E (Msi)
1	-	-	-	0.007	58	10.6	1	-	-	-	0.010	60	13.3
2	-	-	-	0.005	57	13.2	2	-	-	-	0.009	59	14.1
3	-	-	-	0.006	58	11.2	3	-	-	-	0.009	60	13.6
Avg. Total	0.006	60	14.8	0.006	58	11.7	Avg. Total	0.009	60	14.8	0.009	60	13.7

### 8.1.3 Tower Module Sidewall Coupon Testing

The thermal/mechanical sidewall laminate is not a typical layup. Inner ply's are oriented to provide superior thermal conductivity along the vertical axis, and the outer ply's are fabric to provide superior strength to meet the requirements of the GLAST project. For this reason, material property data and joint strength data are not readily available. Material properties, shearout, and pullout coupon testing was performed for two separate materials. A P30 C-C sidewall material was compared to the YS-90A/Ce. The P30 C-C has superior conductivity values, reducing the maximum tower module  $\Delta T$ . The YS-90A/Ce has superior strength at the expense of a higher temperature drop on the tower. The measured material properties for the GLAST sidewall laminates are listed in Table 22. The measured properties for YS-90A/CE are in question for the  $0^\circ$  direction and is being investigated.

**Table 22. Measured Material Properties for the GLAST Sidewall Laminate.**

	P30 C-C		YS-90A/Ce	
	Measured	Predicted	Measured	Predicted
<b>Elastic Modulus (Msi)</b>				
0° Direction (Thrust)	34.8	33.0	35.8	33.4
90° Direction (Transverse)	16.0	15.2	20.7	19.8
<b>Tensile Strength (ksi)</b>				
0° Direction (Thrust)	46.7	44.3	82.1	76.6
90° Direction (Transverse)	27.3	26.1	56.1	53.7
<b>Thermal Conductivity</b>				
0° Direction (Thrust)	309.0	318.0	257.0*	185.0
90° Direction (Transverse)	196.0	192.0	122.0	123.0

\* Value is in question

A series of shearout and pullout tests were performed on both materials to measure the fastener/insert strength allowables. Tests were performed on both materials with and without metallic inserts included. Table 23 lists the results of these coupon tests. It is clear from these results that the YS-90A/CE panels will be capable of carrying the launch loads without the use of metallic inserts. P30 C-C panels will require metallic inserts.

**Table 23. Measured Shearout and Pullout Strengths for the GLAST Sidewall Laminate.**

	P30 C-C		YS-90A/Ce	
	0°	90°	0°	90°
<b>Shearout Strength (N)</b>				
w/insert	1290	1446	1817	1945
w/out insert (avg)	482	545	1323	1400
<b>Pullout Strength (N)</b>				
w/insert (avg)	645		1441	
w/out insert (avg)	191		578	

## 8.2 Subsystem Level Prototype Testing

### 8.2.1 Tray Level Prototype Testing

*References: LAT-SS-00047*

Tray level prototype testing is to be done to the qualification testing specifications set in document # LAT-SS-00047. Three types of tests will be performed on individual tray prototypes: thermal cycling, vibration, and vacuum. Table 24 shows the test to be performed.

**Table 24. Proposed Test Plan for the Tray Prototype.**

No.	Test Description	Purpose
1	Build Prototype Tray	For qualification level testing
2	Sine Sweep using PRISM	Monitor for damage and determine fundamental freqs.
3	Qualification Level Thermal Cycling	Step tray through thermal damage cycling
4	Sine Sweep using PRISM	Monitor for damage and determine change in fundamental freqs.
5	Qualification Level Vacuum Testing	Step tray through vacuum damage cycling
6	Sine Sweep using PRISM	Monitor for damage and determine change in fundamental freqs.
7	Attach Payload to Prototype Tray	Measure tray & payload interaction to testing
8	Sine Sweep using PRISM	Monitor for damage and determine fundamental freqs.
9	Qualification Level Thermal Cycling	Step tray through thermal damage cycling
10	Sine Sweep using PRISM	Monitor for damage and determine change in fundamental freqs.
11	Acceptance Level Random	Step RV inputs to test levels
12	Sine Sweep (or comparable)	Monitor for damage and determine change in fundamental freqs.
13	Acceptance Level Sine Burst	Step SB inputs to test levels
14	Sine Sweep (or comparable)	Monitor for damage and determine change in fundamental freqs.
15	Qualification Level Random	Step RV inputs to test levels
16	Sine Sweep (or comparable)	Monitor for damage and determine change in fundamental freqs.
17	Qualification Level Sine Burst	Step SB inputs to test levels
18	Sine Sweep (or comparable)	Monitor for damage and determine change in fundamental freqs.

### 8.2.2 Tower Level Prototype Testing

A series of TKR tower level prototype testing is scheduled prior to the E/M prototype fabrication begins. These tests are designed to test workmanship and design choices to the launch environment at qualification levels. Performing these tests prior to E/M prototyping will allow design concepts to be tested at qualification levels, with plenty of time to make modifications as needed.

The current program plan calls for the fabrication of five prototype trays and 14 mass simulators. Three standard trays, one top tray, and one bottom tray will be fabricated. The tray prototypes will be populated with dummy silicon, mechanically representing the flight trays. A single 19 tray tower will be constructed using these prototype trays and mass simulators. Mechanical fit alignment tests will be performed to ensure the tower stacking methods meet alignment requirements.

A series of qualification tests will be performed to verify both the workmanship and mechanical performance of the TKR tower. These tests will measure the random vibration, static and thermal response of the TKR tower, and will be compared to FEA. Table 25 lists a proposed test plan, as of PDR. Current expectations are to begin mechanical alignment checks in late July, followed by the random vibration, static, and thermal tests at the end of FY'01.

**Table 25. Proposed Test Plan for the TKR Tower Prototype.**

No.	Test Description	Purpose
1	Measure Tower Alignment <i>Transverse Axis</i>	Verify alignment requirements are met
2	Sine Sweep (or comparable)	Baseline TKR Tower fundamental frequencies
3	Low Level Random	Verify RV inputs and controls are correct and operational
4	Low Level Sine Burst	Verify SB inputs and controls are correct and operational
5	Sine Sweep (or comparable)	Monitor for damage through change in fundamental frequencies
6	Acceptance Level Random	Step RV inputs to test levels
7	Sine Sweep (or comparable)	Monitor for damage through change in fundamental frequencies
8	Acceptance Level Sine Burst	Step SB inputs to test levels
9	Sine Sweep (or comparable)	Monitor for damage through change in fundamental frequencies
10	Qualification Level Random	Full-scale RV test of TKR tower module
11	Sine Sweep (or comparable)	Monitor for damage through change in fundamental frequencies
12	Qualification Level Sine Burst	Full-scale SB test of TKR tower module
13	Sine Sweep (or comparable)	Monitor for damage through change in fundamental frequencies
	<i>Thrust Axis</i>	
14	Sine Sweep (or comparable)	Baseline TKR Tower fundamental frequencies
15	Low Level Random	Verify RV inputs and controls are correct and operational
16	Low Level Sine Burst	Verify SB inputs and controls are correct and operational
17	Sine Sweep (or comparable)	Monitor for damage through change in fundamental frequencies
18	Acceptance Level Random	Step RV inputs to test levels
19	Sine Sweep (or comparable)	Monitor for damage through change in fundamental frequencies
20	Acceptance Level Sine Burst	Step SB inputs to test levels
21	Sine Sweep (or comparable)	Monitor for damage through change in fundamental frequencies
22	Qualification Level Random	Full-scale RV test of TKR tower module
23	Sine Sweep (or comparable)	Monitor for damage through change in fundamental frequencies
24	Qualification Level Sine Burst	Full-scale SB test of TKR tower module
25	Sine Sweep (or comparable)	Monitor for damage through change in fundamental frequencies
	<i>Verify Alignment</i>	
26	Measure Tower Alignment	Check tower for movement during RV and SB tests
27	Measure Fastener Torque	Check fasteners to verify torque requirement is sufficient
	<i>Thermal</i>	
28	Tower/Grid CTE Mismatch	Verify flexure design concept
29	Sine Sweep (or comparable)	Monitor for damage through change in fundamental frequencies
30	Thermal Cycling	Verify TKR tower module to thermal cycling

## 9. Cost for Tracker Tower Mechanical Components

The flight tray mechanical component costs have been reduced significantly since the NASA proposal, Nov. '99, was submitted. These savings can be attributed to several key elements. The closeout frame design concept has been simplified in an effort to reduce engineering development costs. The core material has been changed to aluminum, also as a cost savings measure. The tray face sheets cost estimate was based on the cost of aluminum face sheets, and has since been changed to Gr/Ce, thus raising the cost. The material prices for the YS-90A sidewall material has gone up substantially since the NASA proposal. This resulted in a significant increase in sidewall cost. With all this change, Table 26 shows the cost savings is still \$332 K, and has not changed much since August '00 cost estimates were obtained.

**Table 26. Cost Breakdown of the TKR Tower Module Mechanical Components.**

<i>Flight Tray Mechanical Components</i>	<b>NASA Proposal</b> (Nov. '99)	<b>PDR</b> (May '01)	<b>Delta</b>
Procure Flight Tray Components	\$1,294,720	\$852,650	\$442,070
<i>C-C Closeouts</i>	900,000	635,530	\$264,470
<i>Face Sheets</i>	36,000	134,640	(\$98,640)
<i>Core</i>	288,000	12,960	\$275,040
<i>Adhesives</i>	12,000	10,800	\$1,200
<i>Radiators</i>	38,720	38,720	\$0
<i>Misc. Pieces</i>	20,000	20,000	\$0
Fab, Assemble Assy Fixtures	\$35,786	\$35,760	\$26
Assemble Flight Tray Structures	\$96,600	\$86,250	\$10,350
Procure Flight Tower Components	\$264,000	\$384,415	(\$120,415)
<i>Tower Walls</i>	70,000	267,015	(\$197,015)
<i>Fasteners</i>	80,000	18,750	\$61,250
<i>Bottom Mounting Flexures and Fasteners</i>	54,000	93,650	(\$39,650)
<i>Thermal Gasket</i>	60,000	5,000	\$55,000
<b>Flight Tray Mechanical Total</b>	<b>\$1,691,106</b>	<b>\$1,359,075</b>	<b>\$332,031</b>

## 10. Program Plan

In August '00 the program plan for TKR mechanical component development was modified in an effort to reduce engineering development costs. The original plan was centered on an analytically intensive development approach to which design issues were identified and subsequently solved using various analytical tools, such as FEA. The new program plan accepted the design concepts current in August '00 and qualified these concepts using prototype testing at the coupon, tray and tower level. Design issues are identified through testing and corrected when necessary. Schedules have been shifted to complete this testing effort in time to dovetail with the E/M prototype testing and CDR.

The current milestones for the completion of the engineering development phase, prior to E/M prototype testing and CDR, are as follows:

Date	Duration (weeks)	Milestone
May 15, 2001	4	Procure Sandwich Structure Core Material
May 16, 2001	4	Procure Fastener Inserts
June 4, 2001	2	Re-Impregnate 3D C-C Material
June 8, 2001	3	Machine Assembly Tooling & Components
June 18, 2001	8	Fabricate Gr/Ce Sidewalls
June 18, 2001	2	Machine Prototype Closeout Frame Components
June 19, 2001	0	Tracker PDR
June 25, 2001	4	Fabricate Tray Mass Simulators
July 2, 2001	1	Install Fastener Inserts
July 9, 2001	1	Parylene Coat Machined Closeout Frame Components
July 16, 2001	4	Assemble Tray Sandwich Structures
July 16, 2001	4	Fabricate Aluminum Sidewalls
July 30, 2001	6	Single Tray Thermal/Mechanical Testing
August 13, 2001	2	Tower Mechanical Assembly & Alignment Testing
August 27, 2001	2	Attach Tray Dummy Payload
September 10, 2001	4	Tower Thermal/Mechanical Testing
October 29, 2001	0	Instrument PDR

As anticipated in August '00, the plan to qualify the TKR mechanical design concepts through a series of prototype tests prior to building the E/M prototype is proving to be extremely beneficial. Machining issues with the 3D C-C material have been uncovered and resolved at a time in the program in which delays are more forgiving to the GLAST program schedule. Continued tray and tower level testing will strengthen the results of the E/M prototype testing.

Overall progress to date on the TKR tower mechanical components has been good, with the exception of delays that resulted from solving unforeseen material issues. We do not foresee any technical issues that cannot be solved during normal development at this point.

## 11. References

1. Biehl, F., *GLAST Tracker Static and Dynamic Analysis*, HTN-102070-0005, April 31, 2001.
2. Conley, P.L., *Space Vehicle Mechanisms*, Structural Composites, Chap. 3, June 1998.
3. *Delta II Payload Planners Guide*, Document # MDC H3224D, The Boeing Company, Huntington Beach, CA, April 1996.
4. *Gamma-ray Large Area Space Telescope (GLAST) Large Area Telescope (LAT) Tracker Detailed Subsystem Specification Level IV*, LAT-SS-00134, Draft, May 8, 2001.
5. *General Environmental Verification Specification for STS & ELV – Payload, Subsystems, and Components*, GEVS-SE Rev. A, System Reliability and Safety Office, Code 302, NASA/Goddard Space Flight Center, Greenbelt, MD 20771-0001, June 1996.
6. *GLAST Science Instruments-Spacecraft Interface Requirements Document*, August 3, 1999.
7. Keating, S., Swensen, E., Ney, S., and Ponslet, E., *Material Selection and Thermal Design for the Tracker Sidewalls of GLAST*, HTN-102050-0026, HYTEC Inc., October 27, 2000.
8. Ney, S., Ponslet, E., and Swensen, E., *Investigation of Compliant Layer in SuperGLAST CTE Mismatch Problem*, HTN-102050-0018, HYTEC Inc., August 3, 2000.
9. Ney, S., Swensen, E., and Steinzig, M., *GLAST Standard Tracker Tray Facesheet Material Selection*, HTN-102060-0004, HYTEC Inc., October 2, 2000.
10. Ney, S., *Thermal Conductivity Comparison of Allcomp versus SGL Material for Tracker Tray Closeout Walls*, HTN-102070-0006, HYTEC Inc., May 7, 2001.
11. Norby, M., *LAT Mechanical Performance Specification*, LAT-SS-00047, November 1, 2000.
12. *Proposal for Gamma Ray Large Area Space Telescope*, SLAC-R-522, Stanford Linear Accelerator Center, Stanford University, Stanford, CA, February 1998.
13. Romero, E., Ney, S., and Swensen, E., CAD drawing of *GLAST Tracker Tray Assembly Procedure*, LAT-DS-00106-01 or 102-TKR-13-6010, HYTEC Inc., March 15, 2001.
14. *Structural Design and Test Factors of Safety for Space Flight Hardware*, NASA Technical Standard, NASA-STD-5001, June 21, 1996.
15. Swensen, E., Ney, S., and Steinzig, M., *Tracker Tray Core Material Selection*, HTN-102060-0001, HYTEC Inc., October 3, 2000.
16. Swensen, E., *CTE Mismatch Summary Report of Current Baseline Design*, HTN-102050-0015, HYTEC Inc., June 1, 2000.